

AD-A033 778

STANFORD UNIV CALIF EDWARD L GINZTON LAB
STUDIES OF TECHNIQUES FOR GENERATION OF VACUUM ULTRAVIOLET AND --ETC(U)
DEC 76

F/G 20/5

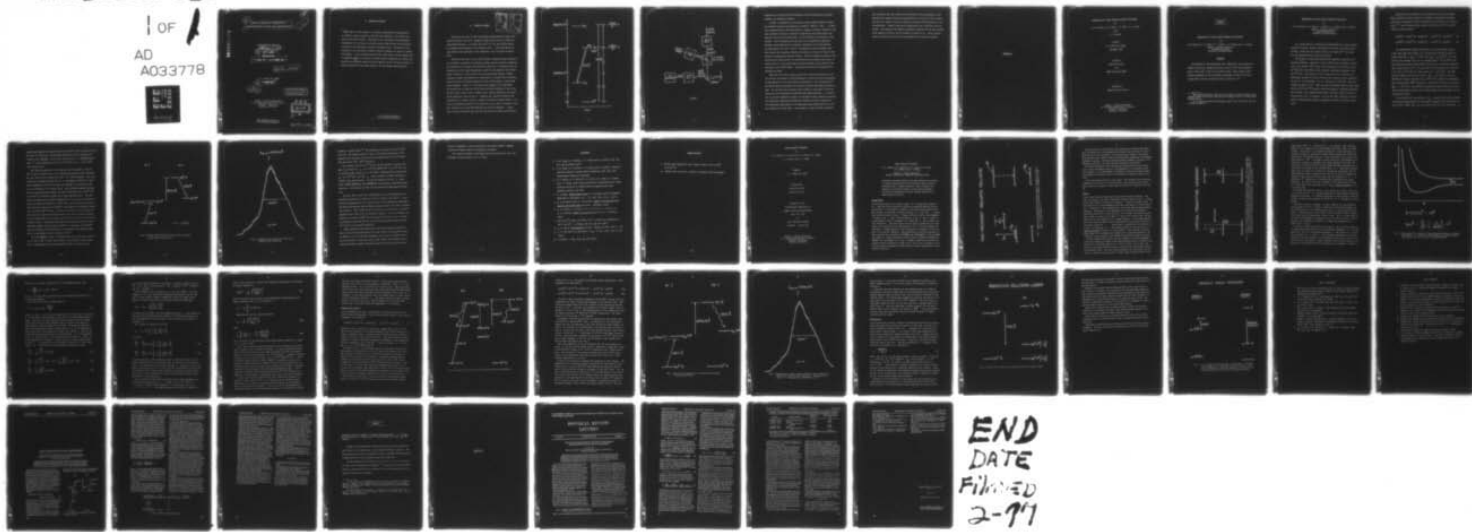
N00014-75-C-0576

NL

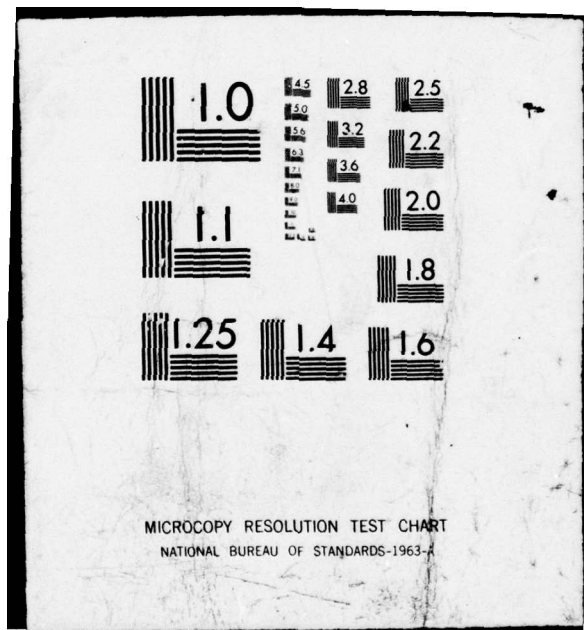
UNCLASSIFIED

GL-2642

1 OF
AD
A033778



END
DATE
Filmed
2-77



MICROCOPY RESOLUTION TEST CHART
NATIONAL BUREAU OF STANDARDS-1963-A

ADA033278

STUDIES OF TECHNIQUES FOR GENERATION OF
VACUUM ULTRAVIOLET AND SOFT X-RAY LASER RADIATION.

B.S.

Office of Naval Research

Contract No 00014-75-C-0576

FINAL REPORT

for the period

1 December 1974 - 30 September 1976.

⑯ GL-2642

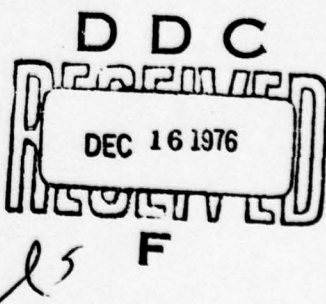
G. L. Report No. 2642

⑮ December 1976

⑯ 49p.

DISTRIBUTION STATEMENT A
Approved for public release;
Distribution Unlimited

Edward L. Ginzton Laboratory
W. W. Hansen Laboratories of Physics
Stanford University
Stanford, California



Copy available to DDC does not
permit fully legible reproduction

409640 AB

I. PROGRAM OBJECTIVES

The goal of this program is to develop techniques for the generation of coherent vacuum ultraviolet and soft x-ray radiation. The overall program has two major thrusts. The first is the theoretical and experimental development of a new type of collision process which we feel has particular promise for the development of short wavelength lasers. The second is the extension of our successful nonlinear optical techniques in vapors to shorter wavelengths. In the following sections work under both of these programs will be summarized. We note that the nonlinear optical techniques are jointly supported by the Advanced Research Projects Agency, and the collision project is jointly supported by the Energy Research and Development Administration.

II. TECHNICAL SUMMARY

ACCESSION NO.	White Series Buff Series	<input type="checkbox"/>	<input type="checkbox"/>
NTIS	REF ID: A64202	<input type="checkbox"/>	<input type="checkbox"/>
STC	SEARCHED	<input type="checkbox"/>	<input type="checkbox"/>
UNCLASSIFIED	INDEXED	<input type="checkbox"/>	<input type="checkbox"/>
DEC 1974	SERIALIZED	<input type="checkbox"/>	<input type="checkbox"/>
FILED		<input type="checkbox"/>	<input type="checkbox"/>
BUREAU OF INVESTIGATION COMM.			
BY			
FBI - BOSTON, MASSACHUSETTS			
A			

During the past year we have successfully demonstrated the first laser induced inelastic collision. Energy was first stored in the Sr $5p^1P^0$ and transferred selectively to either the Ca $4p^2\ ^1S$ or to the Ca $5d^1D$ states, by changing the wavelength of the switching laser. A full description of this work has been published in the literature, and is attached as Appendix A.

During the past year we have used nonlinear frequency mixing techniques in an attempt to generate the coherent, extreme vacuum ultraviolet radiation. Our approach was to enhance the conversion efficiency of a mixing process by choosing two of the input frequencies so that the sum equaled a non-allowed atomic transition. We chose Ne as the nonlinear medium because resonant two-photon pumped sum generation is simplified by a natural near coincidence of the Ne $2p-3p$ non-allowed transition and the 16th harmonic of the Nd:YAG laser frequency. Figure 1 is an energy level diagram of our experiment. The possibility of using the 7th and the 9th Nd:YAG harmonics to sum to the Ne $2p-3p$ level, rather than a tunable source, greatly simplifies the experimental apparatus, shown in Fig. 2. Although this approach eliminates the complexities of tunable sources, a number of technical problems remain: the lack of transparent materials in the VUV; the need to work in vacuum or inert gas; and the lack of good VUV detectors and optical components. A great deal of effort during the past year has been directed towards the efficient

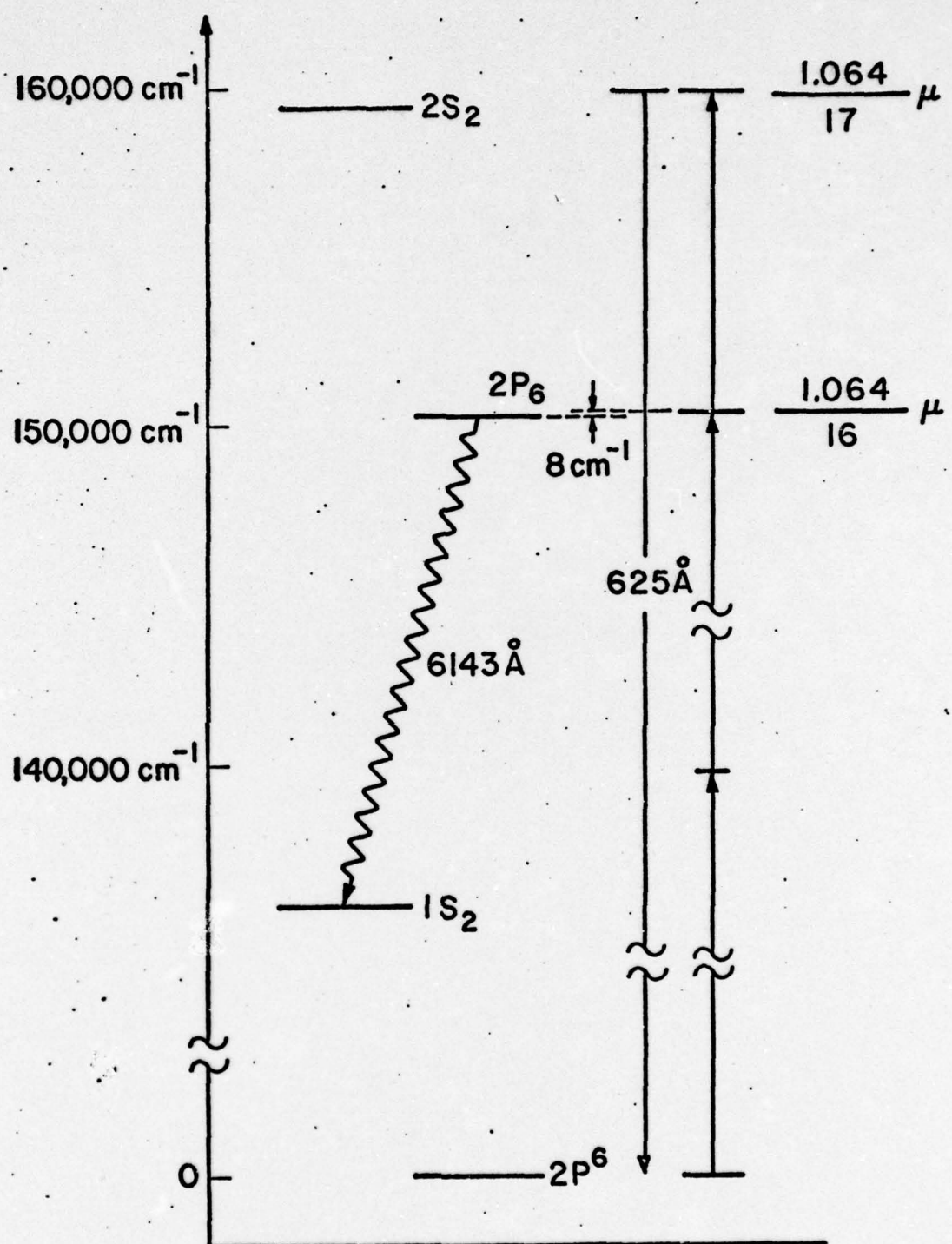


FIGURE 1

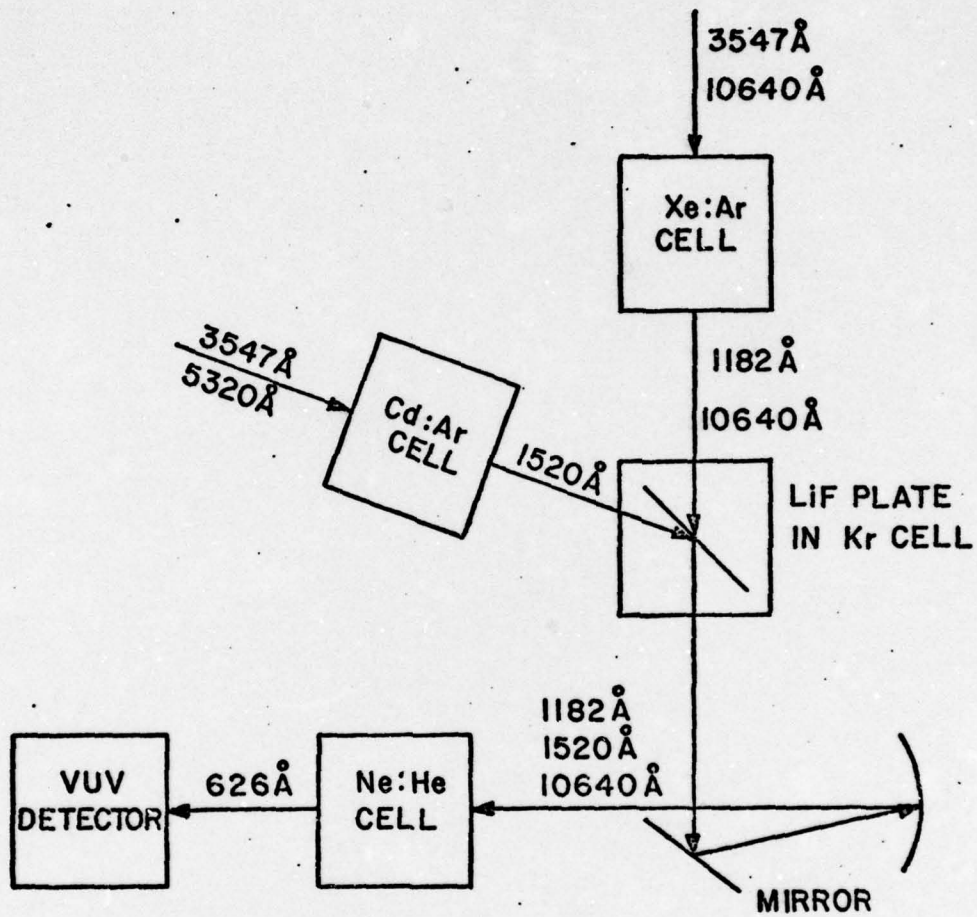


FIGURE 2

combination of 1520 Å and 1182 Å radiation, and the monitoring of spatial, temporal, and frequency overlaps.

A number of attempts have been made to observe 625 Å radiation induced by resonantly enhanced sum generation of 1182 Å + 1520 Å + 1.06 μ. To date, these experiments have been unsuccessful, largely, we believe, because of the great technical difficulty involved in maintaining the proper spatial and temporal overlap of the three beams. We have pursued two solutions to this problem. First we improved the stability of our experimental apparatus. Secondly, the problem would be virtually eliminated if we could generate the 8th harmonic of 1.06 μ, 1330 Å. Two photons of this wavelength alone will produce the resonantly enhanced nonlinearity, without the need for combining and aligning two separate sources. Previous attempts to generate this radiation were unsuccessful, but measurements have indicated that traces of vacuum pump oil in our system have produced extremely strong, selective absorptions in the 1330 Å region. System modifications have eliminated this absorption problem.

Near the end of this contract period the successful generation of the 5th and the 7th harmonic of 2660 Å radiation in both Ne and He was announced by John Reintjes at the Naval Research Laboratories. The resulting 532 Å and 380 Å radiation represents the shortest coherent wavelengths produced to date. We note that this excellent work is based in large part on the techniques and theory developed at Stanford under ONR sponsorship. In particular, Dr. Harris examined the theory of such higher order nonlinear processes, and showed that significant efficiencies should be possible (Appendix B). The preliminary measurements of the NRL group agree qualitatively well with the predictions of this paper. Our attempts to repeat the NRL experiments

have indicated that laser beam profile distortions were preventing us from obtaining the required high peak power densities over the full focal region. This may also explain in part our failure to observe 625 Å previously in the Ne experiments. Careful beam profile measurements and corrections were performed. Our subsequent preliminary experiments indicate that we have successfully generated 532 Å as the 5th harmonic of 2660 Å in He. Further experiments to improve and confirm these measurements are presently underway.

APPENDIX A

OBSERVATION OF LASER INDUCED INELASTIC COLLISIONS

by

R. W. Falcone, W. R. Green, J. C. White, J. F. Young,

and

S. E. Harris

Preprint

G. L. Report No. 2615

September 1976

Contracts

N00014-75-C-0576

and

ERDA E(04-3)-326-PA#41

submitted to

Physical Review Letters

Edward L. Ginzton Laboratory
W. W. Hansen Laboratories of Physics
Stanford University
Stanford, California

COMMENT

OBSERVATION OF LASER INDUCED INELASTIC COLLISIONS *

by

R. W. Falcone, W. R. Green,[†] J. C. White, J. F. Young, and S. E. Harris
Edward L. Ginzton Laboratory
Stanford University
Stanford, California 94305

Abstract

We describe two new experiments which demonstrate laser induced inelastic collisions. Energy was stored in the Sr $5p^1P^0$ and transferred both to the Ca $4p^2\ 1S$ and to the Ca $5d^1D$ states. The collision cross sections maximized at the interatomic wavelengths of $4977\ \text{\AA}$ and $4711\ \text{\AA}$ respectively, and had a half-power width of about $14\ \text{cm}^{-1}$.

* This work was jointly supported by the Office of Naval Research under contract number N00014-75-C-0576 and by the Energy Research and Development Administration.

† W. R. Green gratefully acknowledges support from the Fannie and John K. Hertz Foundation.

OBSERVATION OF LASER INDUCED INELASTIC COLLISIONS

by

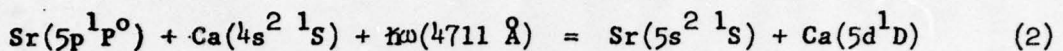
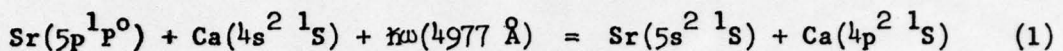
R. W. Falcone, W. R. Green, J. C. White, J. F. Young, and S. E. Harris

Edward L. Ginzton Laboratory
Stanford University
Stanford, California 94305

In a recent Letter¹ we reported the demonstration of a laser induced inelastic collision; further investigations, however, have shown that an artifact, rather than the reported effect, was observed.^{2,3} We report two new experiments which avoid this problem.

The signals we observed previously were apparently produced by the following sequence: population of the Sr $4d\ ^3D_3$ level, probably by quenching of the pumped Sr $5p\ ^1P^0$ state; laser excitation at 6408.5 \AA to the Sr $5p'\ ^3F_4^0$ state; and finally normal inelastic collisional transfer to the Ca $4d\ ^1D$ level. The resolution of our experiment was not sufficient to distinguish between this process and the laser induced transfer predicted to occur at the interatomic ($R = \infty$) wavelength of 6408.6 \AA . (All wavelengths are given in air.) When we tuned the transfer laser to other lines in the Sr $4d\ ^3D - 5p'\ ^3F^0$ series we observed signals of comparable magnitude and lineshape, thus confirming that such an artifact, rather than the reported effect, had been observed. We note that these processes exhibited narrow linewidths which pressure broadened as expected for atomic transitions.

Recently we have performed two new experiments in the Sr-Ca system which eliminate the above artifact by avoiding a wavelength coincidence between the interatomic transfer wavelength and any known Sr or Ca transitions.⁴⁻⁶ Laser induced energy transfer to both the Ca $4p^2 1S$ and $5d^1 D$ states has been observed:⁷



The experimental details were similar to those described in Ref. 1. A heat pipe type cell provided a ~ 3 cm long zone of Sr and Ca vapor at atomic densities of $N_{Sr} = 4 \times 10^{16}$ and $N_{Ca} = 6 \times 10^{15} \text{ cm}^{-3}$, as determined by the resonance line curve of growth method.⁸ The Sr $5p^1 P^0$ level was populated by direct single photon absorption of a flashlamp-pumped dye laser tuned about 50 cm^{-1} to the red side of the resonance line, focussed to an area of 10^{-3} cm^2 and a power density of $1 \times 10^4 \text{ W/cm}^2$. The radiatively trapped, excited state density, N_{Sr}^* , was determined using a 6357 \AA probe laser to saturate the Sr $5p^1 P^0 - 7s^3 S$ transition and measuring the resulting $7s^3 S - 5p^3 P^0$ fluorescence. The measured density was typically $N_{Sr}^* = 3 \times 10^{13} \text{ cm}^{-3}$, and should be considered an upper bound, since collisional quenching could reduce the Sr $5p^1 P^0$ population in the absence of the strong probe field.

The excited state Ca population, N_{Ca}^* , produced by the laser induced collisional energy transfer was determined by measuring the fluorescence of the Ca $4p^2 1S - 4p^1 P^0$ [Eq. (1)] or Ca $5d^1 D - 4p^1 P^0$ [Eq. (2)] transitions. An

energy level diagram for transfer into the Ca $4p^2 1S$ level is shown in Fig. 1.

The ratio of the Ca to Sr fluorescence signals was used to determine the transfer ratio N_{Ca}^*/N_{Sr}^* , and thus the cross section $\sigma_c = (N_{Ca}^*/N_{Sr}^*)/N_{Ca}\bar{V}\tau$, where \bar{V} is the average velocity (9×10^4 cm/sec), and τ is the laser pulse length (1 μ s).

The relative magnitude of the cross section for transfer to the Ca $4p^2 1S$ level is shown in Fig. 2 as a function of transfer laser wavelength; the curve has not been corrected for the 2 cm^{-1} laser linewidth. The cross section has a maximum at about the $R = \infty$ wavelength of 4976.8 \AA , a half-power linewidth of 14 cm^{-1} , and drops less rapidly for red detuning than for blue detuning of the transfer laser. This lineshape remained constant when the argon buffer gas density was varied from about 10^{17} to 10^{18} cm^{-3} , in contrast to "artifact" signals of the type described above. The lineshape and position also remained unchanged as the pump laser wavelength was tuned both above and below the Sr $5p^1 P^0$ level, thus eliminating the possibility that the signals were produced by quasi-molecular two-photon absorption into the Ca $4p^2 1S$ state. We have also examined the possibility that the signals are caused by two-photon absorption, with one photon provided by the transfer laser, and a second by spontaneous fluorescence from the Sr resonance level. Calculations show that such a process would be at least 1000 times weaker than the signals observed. In addition, the observed constant linewidth and red asymmetry is inconsistent with the known asymmetric Ar broadening of the Sr resonance level.⁹

The red asymmetry in Fig. 2 indicates that the van der Waals constant C_6 for the Ca $4p^2 1S$ state exceeds that for the Sr $5p^1 P^0$ storage state; this is consistent with a rough calculation based on large Ca matrix

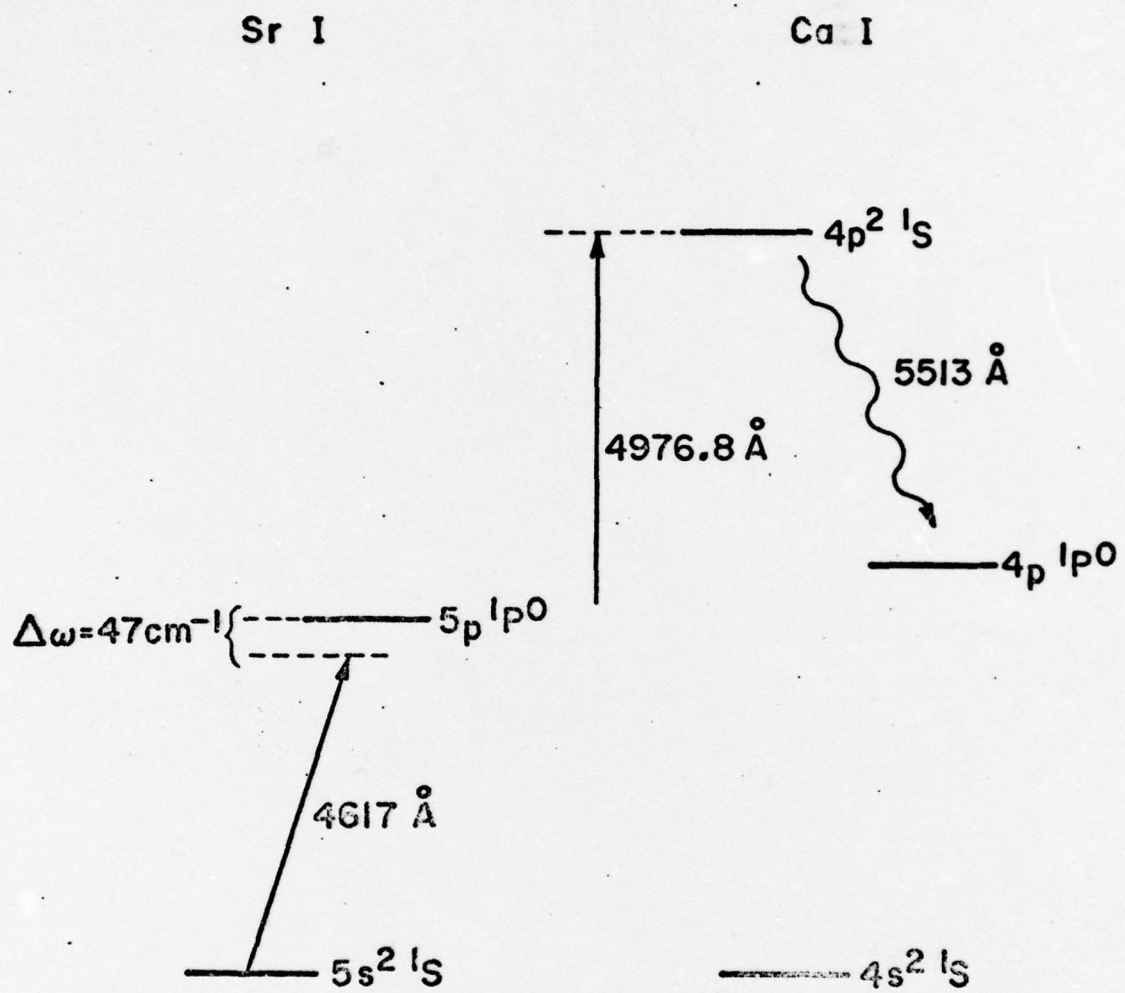


Fig. 1--Energy level diagram for laser induced transfer
from Sr $5p^1P^0$ to Ca $4p^2 1S$.

$$\lambda_{R=\infty} = 4976.8 \text{ \AA}$$

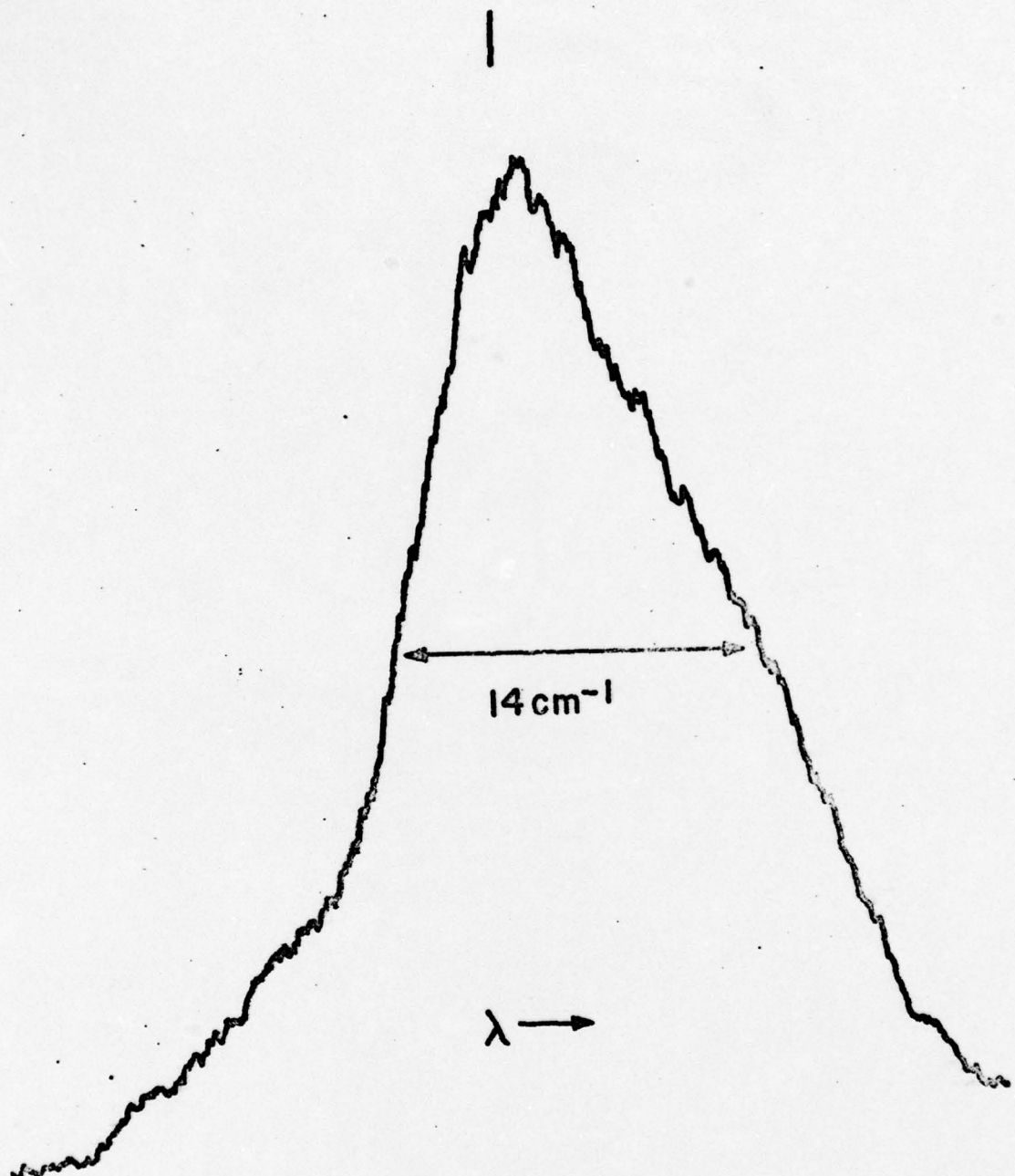


Fig. 2--Induced cross section as a function of transfer laser wavelength.

elements to nearby states.¹⁰ The lineshape for transfer into the Ca 5d¹D state [Eq. (2)] appears similar to Fig. 2, but precise evaluation is not possible since the wing is distorted by an adjacent peak at 4714 Å associated with the Sr 4d³D - 7p³P⁰ transition.

For transfer into the Ca 4p² 1S level theory predicts a velocity averaged cross section of $\sigma_c = 9 \times 10^{-23} \text{ P/A (W/cm}^2\text{)} \text{ cm}^2 = 5 \times 10^{-17} \text{ cm}^2$ for our transfer power density of $5 \times 10^5 \text{ W/cm}^2$. Experimentally we found that $\sigma_c = 9 \times 10^{-18} \text{ cm}^2$, and that σ_c varied linearly for small variations of transfer laser power density. We feel the measured value of σ_c represents a good lower bound, and experimental uncertainties, especially number densities, can reasonably account for the theoretical-experimental discrepancy.

We would like to note that considerable care in the adjustment of experimental parameters is required in order to observe this effect. In particular, background noise (no transfer laser) at the observation wavelength increased quadratically with increasing pump power while the signal increased only linearly. The Sr 5p¹P⁰ density was chosen to provide both a reasonable signal-to-noise ratio (~ 5) and detectable signals. For our conditions, the signals are typically 1/50th of that obtained by tuning the transfer laser to a frequency such that the sum of it plus the pump laser excites the Ca 4p² 1S level by two-photon absorption.

These experiments have shown that laser induced transfer provides a means of selectively directing stored atomic energy into particular states. In addition, the cross section lineshapes can be used to determine interatomic potentials. Topics for future study include laser induced spin exchange and charge exchange collisions; these processes should have cross

sections comparable to that reported here, but should exhibit a maximum considerably shifted from the interatomic wavelength.

The authors gratefully acknowledge helpful discussions with Drs. Alan Gallagher, Sidney Geltman, and M. G. Payne.

REFERENCES

1. D. B. Lidow, R. W. Falcone, J. F. Young, and S. E. Harris, Phys. Rev. Lett. 36, 462 (March 1976).
2. D. B. Lidow, R. W. Falcone, J. F. Young, and S. E. Harris, "Inelastic Collision Induced by Intense Optical Radiation," Phys. Rev. Lett. (simultaneous submission) [Erratum].
3. S. E. Harris, R. W. Falcone, W. R. Green, D. B. Lidow, J. C. White, and J. F. Young, "Laser Induced Collisions," Proceedings of the International Conference on Tunable Lasers and Applications, Loen, Nordfjord, Norway, June 1976.
4. C. E. Moore, Atomic Energy Levels, U.S. National Bureau of Standards NSRDS-NBS 35 (Washington, D.C.: U.S. GPO, 1971), Vols. I and II.
5. A. R. Striganov and N. S. Sventitskii, Tables of Spectral Lines of Neutral and Ionized Atoms (New York: IFI/Plenum, 1968).
6. A. N. Zaidel', V. K. Prokf'ev, S. M. Raikii, V. A. Slavni, and E. Ya. Shreider, Tables of Spectral Lines (New York: IFI/Plenum, 1970).
7. The Ca $4p^2$ 1S state, at 41786.3 cm^{-1} , is incorrectly designated in Ref. 4 as $6s^1S$. G. Risberg, Ark. Fys. 37, 231 (1968).
8. A. P. Thorne, Spectrophysics (London: Chapman and Hall, 1974), p. 307.
9. J. M. Farr and W. R. Hindmarsh, J. Phys. B: Atom. Molec. Phys. 4, 568 (1971).
10. G. McGinn, J. Chem. Phys. 51, 5090 (1969).

FIGURE CAPTIONS

1. Energy level diagram for laser induced transfer from Sr $5p^1 P^0$ to Ca $4p^2 ^1 S$.
2. Induced cross section as a function of transfer laser wavelength.

LASER INDUCED COLLISIONS

by

S. E. Harris, R. W. Falcone, W. R. Green, D. B. Lidow,
J. C. White, and J. F. Young

Preprint

G. L. Report No. 2577

Contract Nos.

N00014-75-C-0576

N00014-75-C-1175

Presented at the
International Conference on
Tunable Lasers and Applications

June 7-11, 1976

at

Loen, Nordfjord, Norway

Prepared: August 1976

Edward L. Ginzton Laboratory
W. W. Hansen Laboratories of Physics
Stanford University
Stanford, California

Laser Induced Collisions *

S. E. Harris, R. W. Falcone, W. R. Green, D. B. Lidow
J. C. White, and J. F. Young

Edward L. Ginzton Laboratory
Stanford University, Stanford, California 94305

We describe processes where one or more photons are utilized to conserve energy between the initial and final states of colliding atoms. Energy transfer is thus initiated, and directed to particular states, by the optical radiation. We report new experiments which we believe demonstrate a laser induced collision.

Introduction

If the energy defect of an atomic process ΔE is large with respect to kT , then the cross section for collision or chemical reaction will be quite small. In this paper we consider collision processes where one or more photons are utilized to conserve energy, i.e., $n\hbar\omega \approx \Delta E$. A prototype system is shown in Fig. 1. Energy is first stored in the designated s state of the A atom. During collision of the A and B atoms an electromagnetic field at frequency $\hbar\omega$ causes the A atom to make a virtual transition. Long range dipole-dipole coupling between the two atoms causes this excitation to be transferred to the B atom to complete the excitation. Energy transfer is thus initiated or "switched" by the presence of the optical radiation. The possibility of collision processes of this type have been predicted by GUDZENKO and YAKOVLENKO [1] and by HARRIS and LIDOW [2]. Recent theoretical work is given by PAYNE and NAYFEH [3], GELTMAN [4], and GEORGE, et al. [5]. Though an apparently successful experiment recently reported by LIDOW, et al. [6] is now in question, we report additional experimental results which we believe demonstrate a laser induced collision.

NON-RESONANT INELASTIC COLLISION

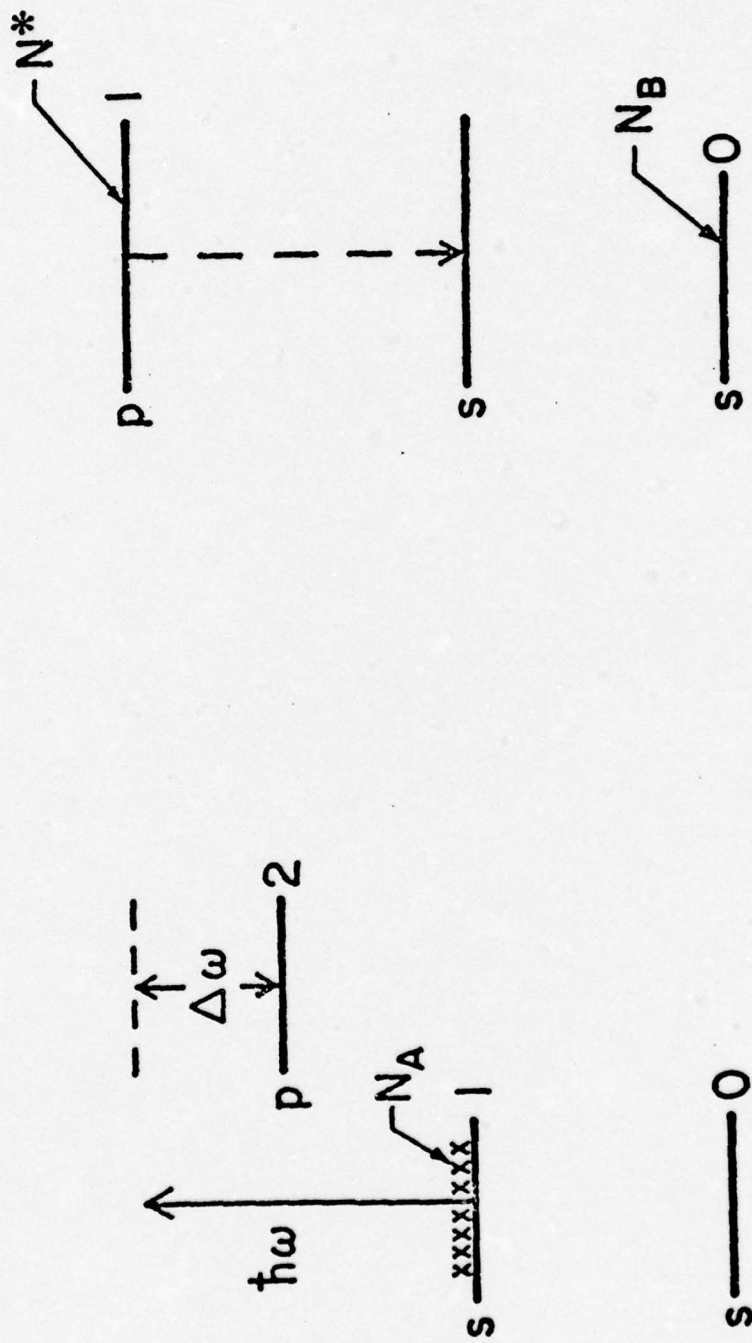


Fig. 1--Schematic of laser induced collision process. Energy is stored in the s state of atom A and may be rapidly transferred to the upper p state of atom B

Optical processes involving the near simultaneous collision and absorption of photons may be considerably more general than that shown in Fig. 1. They may involve the absorption of several photons instead of one photon. They may take place between states involving dipole-quadrupole or quadrupole-quadrupole coupling. Processes involving charge exchange collisions, spin exchange collisions, and even free-bound reactions are possible.

Collision processes of this type may have application to the construction of short wavelength lasers, to the mapping out of interatomic potential surfaces, to the development of radiative collision and Raman lasers and frequency converters, and to the initiation of selected chemical reactions.

In the following sections of this paper I will describe these processes, summarize the theory as it is known to date, and describe recent experiments wherein we observed a laser induced collision in a mixture of Sr and Ca.

Theory

I will first describe these effects from three related viewpoints. The first of these is the virtual transition viewpoint shown in Fig. 2. Assume first, that energy is stored in an excited s state of the first atom. In the presence of an electromagnetic field this atom makes a virtual transition. Excitation is then transferred to the second atom via dipole-dipole coupling. The process is thus described as a virtual electromagnetic transition followed by a real collision. Now consider the reverse process where energy is stored in the upper p level of the second atom, and radiation at the same frequency $\hbar\omega$ is again present. As the atoms approach each other they each make virtual transitions in the opposite direction to the arrows denoted by 2. The process is completed by the emission of a photon of frequency $\hbar\omega$. The overall process is thus described as a virtual collision followed by a real emission. For collision velocities high enough that a straight-line trajectory is a good approximation, the collision cross sections for the forward and reverse processes are equal.

We next consider the process from the viewpoint of an electromagnetic transition between the states of the quasi-molecule which is formed during the time of a collision between an A and B atom. Fig. 3 shows the energy of the quasi-molecular state as a function of the distance between the colliding atoms. The lower state represents the sum energy of an excited A atom and a ground state B atom, while the upper state is the

VIRTUAL TRANSITION VIEWPOINT

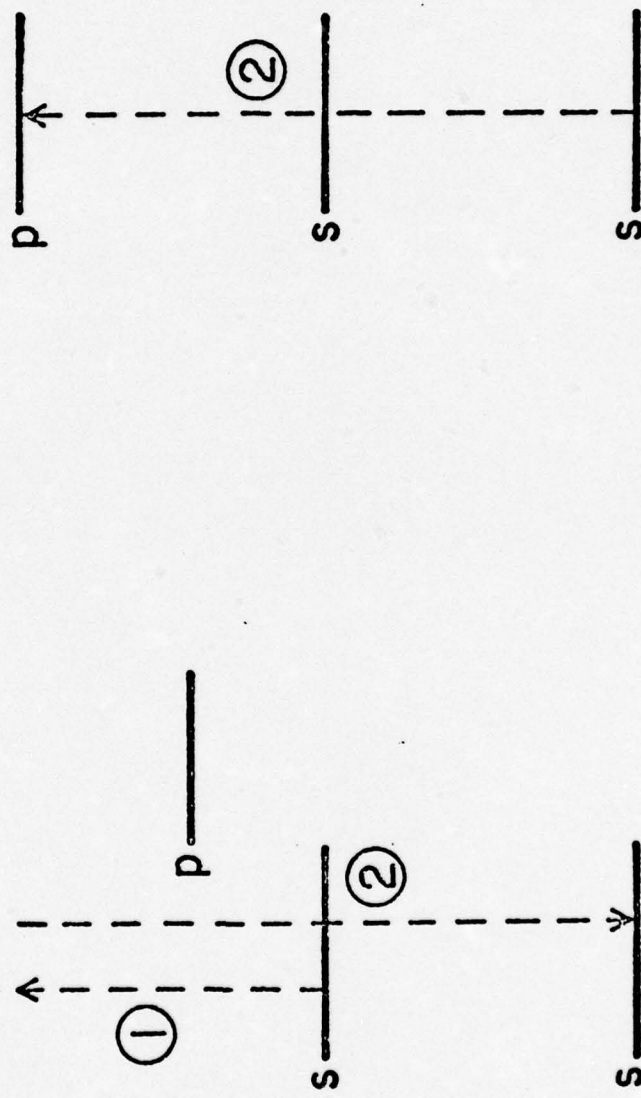


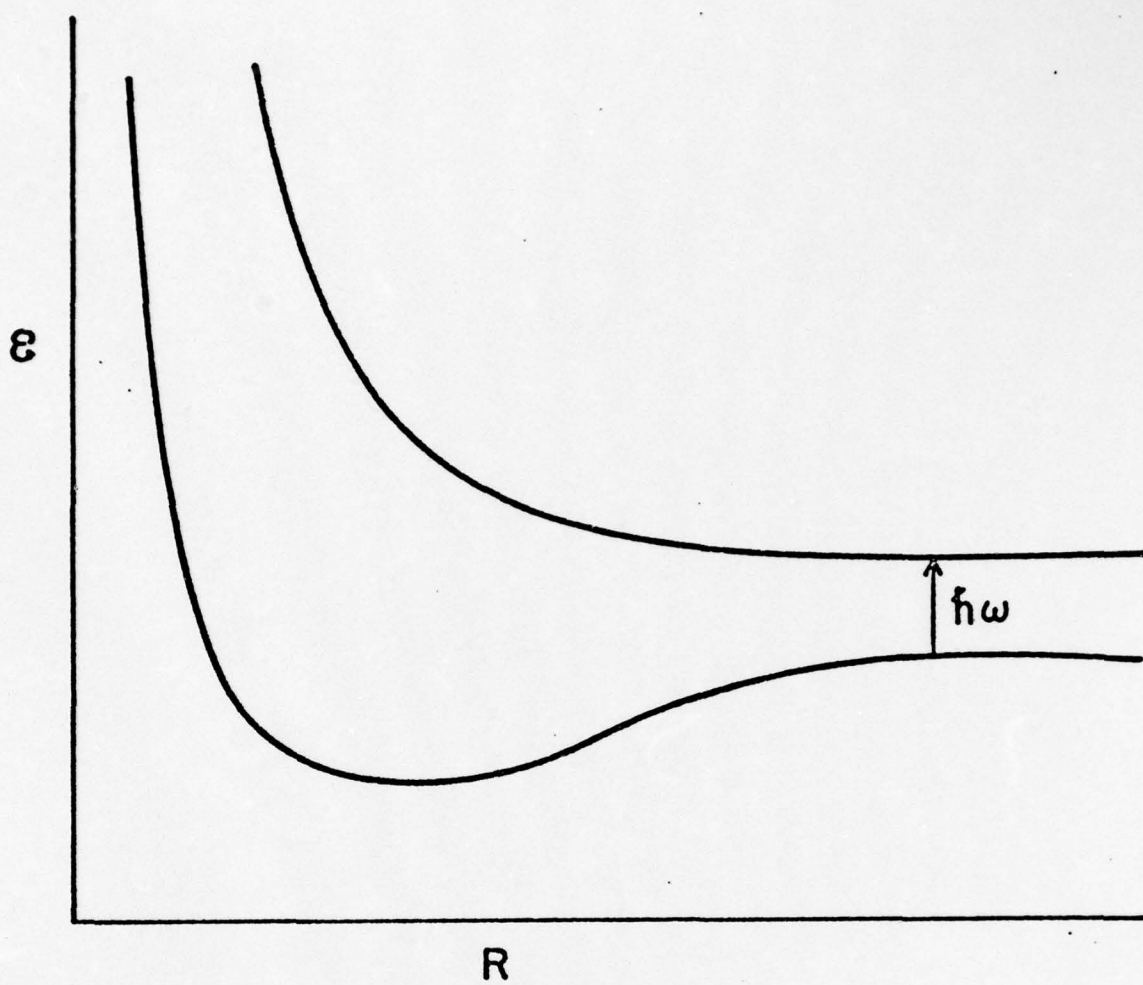
Fig. 2--Virtual transition viewpoint of laser induced collisions. For flow of energy from the left- to the right-hand atom, the process is best considered as a virtual electromagnetic transition followed by a real collision. For the reverse process, we view the process as a virtual collision followed by a real transition.

final state, where B is excited and A is at ground. This viewpoint leaves out the dynamics of the intermediate state and is thus not always correct. In any case it is somewhat misleading. Using stationary perturbation theory one calculates a matrix element between the initial and final states of the quasi-molecule. Since the square of this matrix element varies as $1/R^6$, one might at first expect the electromagnetic absorption to increase in strength as the atoms approach each other, and thus expect a broad linewidth (at least several hundred wavenumbers) as a function of the energy of the incident photon ν . More exact analysis shows that the square of the effective interaction time between the colliding species varies inversely as the slope of the relative energy difference of the initial and final states and thus increases as R^7 . An additional R^2 dependence is introduced when integrating over impact parameter. We will see that the linewidth for the dipole-dipole process is in fact quite narrow and peaks at the $R = \infty$ energy separation of the colliding atoms.

Following the reasoning of Fig. 3, one expects the collision cross section to peak at the $R = \infty$ energy separation for dipole-dipole and dipole-quadrupole processes. For quadrupole-quadrupole, spin exchange, charge exchange, and free-bound processes a peak at the $R = \infty$ frequency is not expected.

The third viewpoint is ad hoc. In this viewpoint the electromagnetic field applied to atom A causes an effective per atom dipole moment at the sum frequency of the energy stored in atom A and the applied field. Each A atom possesses a near electric field often many orders of magnitude larger than the macroscopic electric field. As an A atom passes a B atom an electromagnetic transition of the B atom is induced. The dephasing event allowing the transition is simply the passage of the A atom by the B atom.

I now give a brief description of the theory. The overall procedure is to apply perturbation theory at fixed interatomic separation R ; to integrate over $R(t)$ for fixed impact parameter ρ and velocity \bar{v} ; and to then integrate over ρ and \bar{v} . The principal assumptions are that the collisions are slow compared to the orbiting velocity of an electron, and that the net energy defect is small compared to the incident energy of the particles, thus implying that the trajectories are unchanged. We work in



$$|\langle 1 | x | 2 \rangle|^2 \sim 1/R^6$$

$$|\Delta t|^2 \sim \left[\frac{1}{V} \frac{1}{\hbar} \frac{1}{\partial \epsilon / \partial R} \right] \sim R^7$$

Fig. 3--Quasi-molecular viewpoint of laser induced collisions. A photon of frequency $\hbar\omega$ causes an electromagnetic transition between the initial and final state of the quasi-molecule.

a basis set of product eigenfunctions of the separated atoms. Thus

$$\psi = \sum_n c_n(t) u_n \exp - jE_n t / \hbar \quad (1)$$

The u_n are the product eigenfunctions of the atomic states and the E_n are the sum energies.

The classical interaction hamiltonian is

$$H' = ex_1 E + ex_2 E + \frac{e^2 x_1 x_2}{R^3} \quad (2)$$

where x_1 and x_2 are the local coordinates of the electrons of each atom, E is the applied electromagnetic field, and R is the distance between atoms. The first two terms represent the interaction of the electromagnetic field with each atom separately while the latter term gives the dipole-dipole coupling between the two atoms. Following the notation of Fig. 1 we assume three pertinent product states. c_1 is the amplitude of the product state whose energy is the sum of the storage s state of the first atom and the ground state of the second atom. c_2 is the amplitude of the p state of atom A and the ground state of atom B, while c_3 is the amplitude of the upper p state of atom B and the ground state of atom A. We consider the on line center case where $\hbar\omega$ = the energy defect ΔE . Substituting into Schrödinger's equation we obtain

$$\frac{\partial c_1}{\partial t} = \frac{1}{j\hbar} \frac{\mu^{A1} E}{2} c_2 \exp j\Delta\omega t \quad (3a)$$

$$\frac{\partial c_2}{\partial t} = \frac{1}{j\hbar} \frac{\mu^{A1} E}{2} c_1 \exp - j\Delta\omega t + \frac{1}{j\hbar} \frac{\mu^{A2} \mu^B}{R^3(t)} c_3 \exp - j\Delta\omega t \quad (3b)$$

$$\frac{\partial c_3}{\partial t} = \frac{1}{j\hbar} \frac{\mu^{A2} \mu^B}{R^3(t)} c_2 \exp j\Delta\omega t \quad (3c)$$

$\Delta\omega$ is the energy separation of the upper p levels, as shown in Fig. 1. μ^{A1} , μ^{A2} , and μ^B are defined as: $\mu^{A1} = \langle 1|x_1|2\rangle^A$, $\mu^{A2} = \langle 2|x_1|0\rangle^A$, and $\mu^B = \langle 1|x_2|0\rangle^B$.

If the relative rate of change of c_1 , c_3 , and $1/R^3(t)$ are slow compared to $\Delta\omega$ then (3b) may be integrated and combined into (3a) and (3c) to yield coupled equations between the initial and final states.

These two coupled states have an effective interaction hamiltonian

$$H_{13} = H_{31} = \left(\frac{\mu^{A1} E}{2\hbar\Delta\omega} \right) \frac{\mu^{A2} \mu^B}{R^3(t)}$$

By varying the strength of the electromagnetic field E , the strength of the interaction hamiltonian may be varied. By varying the frequency of the electromagnetic field an effective curve crossing may be created at arbitrary R .

By a change of variable of the form

$$c_i = a_i \exp \left[-\frac{j}{\hbar} \int_{-\infty}^t \frac{c_6}{R^6(t)} dt \right]$$

(3) become

$$\frac{\partial a_1}{\partial t} = \frac{H_{13}}{j\hbar} a_3 \exp \left[-\frac{j}{\hbar} \int_{-\infty}^t \frac{c_6}{R^6(t)} dt \right] \quad (4a)$$

$$\frac{\partial a_3}{\partial t} = \frac{H_{13}}{j\hbar} a_1 \exp \left[\frac{j}{\hbar} \int_{-\infty}^t \frac{c_6}{R^6(t)} dt \right] \quad (4b)$$

In these equations I have neglected a small ac Stark shift which for the power densities which we will consider will be (at most) a few tenths of a cm^{-1} . The (relative) van der Waals constant c_6 includes not only terms which come directly from (3), but also all other contributions pertinent to the difference of the energy shifts between the initial and final states. This shift is quite important and sets the minimum impact parameter which contributes to the interaction.

We now examine the weak-field case where for all impact parameters we may neglect the depletion of a_1 . We take $R(t) = [\rho^2 + \frac{V^2}{\lambda^2} t^2]^{\frac{1}{2}}$.

We assume a constant impact parameter ρ and integrate (4b) over $t = -\infty$ to $t = +\infty$. For impact parameters such that the exponent in

(4b) is less than about 1 radian, the transition probability as a function of impact parameter is

$$|a(\rho)|^2 = \frac{1}{\hbar^4} \left(\frac{\mu^{A_1} \mu^{A_2} B}{\Delta\omega \sqrt{\rho}} \right)^2 \quad (5)$$

The cross section for collision is now obtained by integrating over all impact parameters from ρ_0 to infinity, or

$$\sigma_c = 2\pi \int_{\rho_0}^{\infty} |a(\rho)|^2 \rho d\rho$$

Combining the above we obtain the result

$$\sigma_c = \frac{\pi}{\hbar^4} \left(\frac{\mu^{A_1} \mu^{A_2} B E}{\sqrt{V \Delta\omega} \rho_0} \right)^2 \quad (6a)$$

where

$$\frac{1}{\hbar} \int_{-\infty}^{+\infty} \frac{c_6}{R^6(t)} dt \approx \frac{3\pi}{8} \frac{|\mu^{A_2}|^2 |\mu^B|^2}{\hbar^2 V \Delta\omega \rho_0^5} = 1 \quad (6b)$$

The second part of (6b) determines the minimum impact parameter ρ_0 which is to be used in (6a).

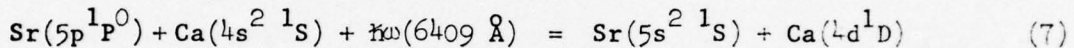
If we assume that all involved transitions have relatively large oscillator strength, then at thermal velocities, ρ_0 will typically be greater than 10 Å and the details of the atomic potentials for small interaction distances need not be considered. For $\Delta\omega \approx 5000 \text{ cm}^{-1}$, typical predicted collision cross sections are about $\sigma_c \approx 5 \times 10^{-23} \frac{P}{A} (\text{W/cm}^2) \text{ cm}^2$. Thus an incident power density of about 1 MW/cm² is required to obtain cross sections of atomic dimension. Though I will not go into detail here, it is expected that the cross section for collision will continue to increase linearly with power density until reaching approximately $\pi \rho_0^2$. We believe that collision cross sections as large as 10^{-13} cm^2 should be obtainable, and experiments to demonstrate such cross sections are underway.

To this point we have considered the cross section for collision induced by a laser tuned to the $R = \infty$ frequency of the separated atoms. The expected line shape as a function of the frequency of the transfer laser is of considerable interest. If it were not for the dependence of the eigenenergies of the quasi-molecular states on the interatomic spacing

then the line shape for transfer would be a first order modified Bessel function of the third kind with argument $(2\pi\Delta f p_0/\sqrt{V})$, where Δf is the frequency defect. For a situation such as that in Fig. 3 where the energy level of the lower quasi-molecular state falls faster than the upper state, a quite rapid fall-off is expected on the low frequency side of the $R = \infty$ frequency. On the high frequency side, the tunable laser in effect causes a curve crossing at arbitrary R . One might intuitively expect a sharp fall off on the red side, and a slowly varying tail on the blue side. Further work - both theoretical and experimental - is necessary.

Experimental Results

In our presentation at Loen, we described a key difficulty with a previously reported experiment. The collision process studied in this earlier experiment is described by



Energy was first stored in the radiatively trapped $5p^1P^0$ level of Sr I. The level was populated by two-photon pumping of the $5d^1D$ Sr level, followed by radiative decay. A second laser at 6409 \AA was used to induce inelastic collision to the $4d^1D$ level of Ca I. The overall process is best viewed as a virtual collisional excitation, followed by a real absorption. For this experiment, $\hbar\Delta\omega = 1954 \text{ cm}^{-1}$, and (6) predicts $p_0 = 16.7 \text{ \AA}$, and $\sigma_c = 2.9 \times 10^{-23} \frac{\text{P}}{\text{\AA}} (\text{W/cm}^2) \text{ cm}^2$.

As shown in Fig. 4, the difficulty with this experiment arises due to the presence of a transition at 6408.5 \AA within the triplet series of Sr. This transition differs by only $.1 \text{ \AA}$ from the interatomic frequency of 6408.6 \AA , and is beneath our resolution. A possible artifact path now consists of collisional transfer from the Sr $5p$ to the Sr $4d^3D$ levels, followed by laser excitation at 6408.5 \AA and collisional transfer to the Ca $4d^1D$ level. The fact that signals of comparable magnitude were observed when the transfer laser was tuned to other lines in the same triplet series, as well as the narrow symmetrical linewidth of the observed signal, indicates that the artifact rather than the true effect was observed.

Following the conference at Loen we succeeded in demonstrating laser induced collisions in the Sr-Ca system, but using two different target

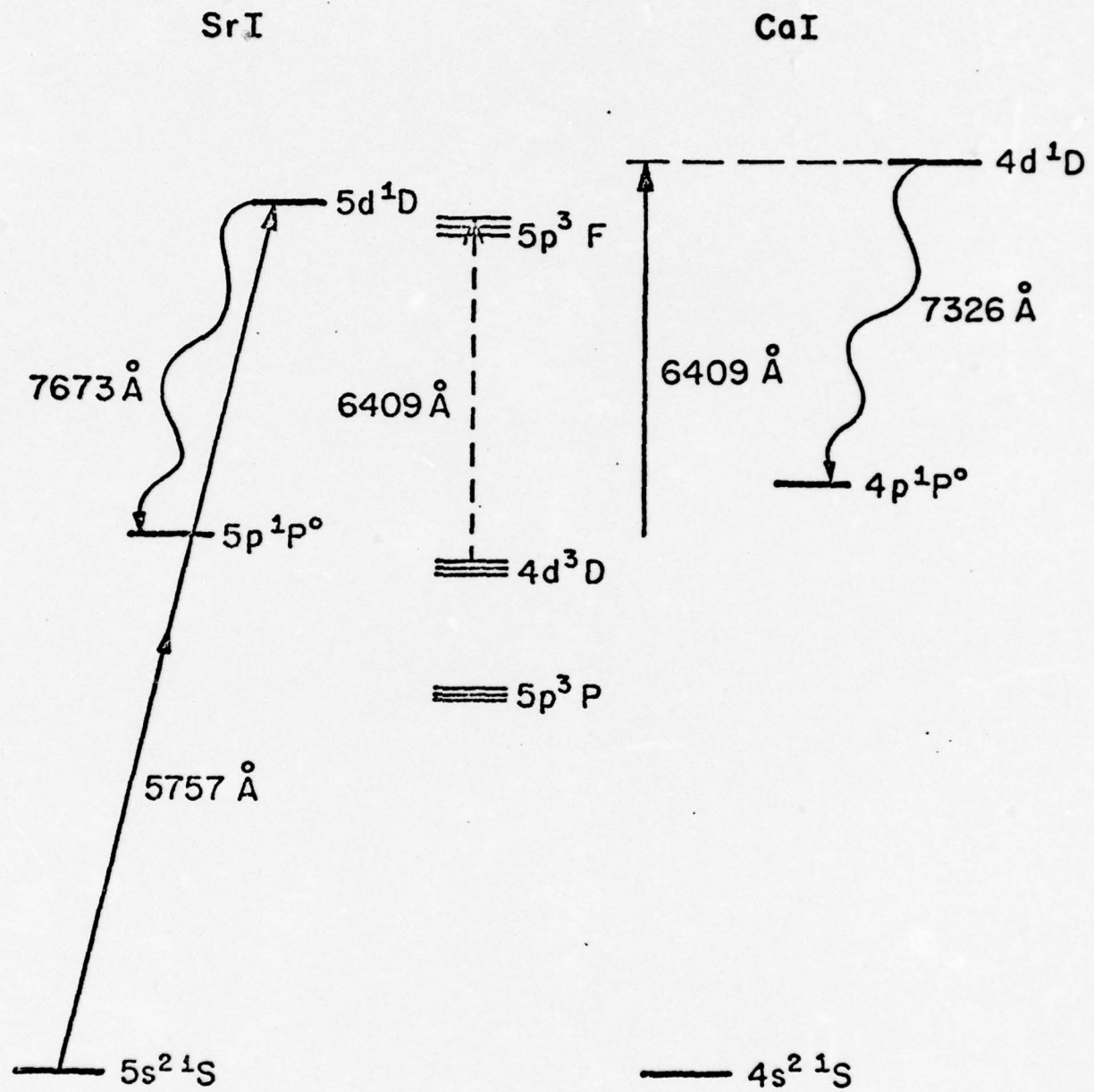
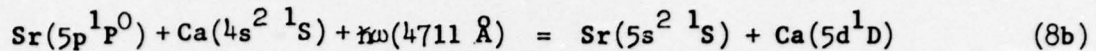


Fig. 1--Energy level diagram for Sr-Ca induced-collision experiment.

states in Ca, i.e., the $\text{Ca}(6s^1S)$ and $\text{Ca}(5d^1D)$ states respectively. These experiments are described by



In both of these experiments pumping of the $\text{Sr}(5p^1P^0)$ storage level was accomplished by direct single photon pumping of the resonance line. Typically this pumping laser was on the red side of the line and was detuned by about 50 cm^{-1} . An energy level diagram for the $\text{Ca}(6s)$ target state experiment is shown in Fig. 5. The power densities of the pumping and transfer lasers were about 10^5 W/cm^2 and 10^6 W/cm^2 respectively. The number density of Sr and Ca was $\sim 10^{15} \text{ atoms/cm}^3$.

Collisional transfer was monitored by examining the fluorescence from the $\text{Ca}(6s^1S)$ to the $\text{Ca}(4p^1P^0)$ state. The amplitude of this fluorescence signal, and thus the magnitude of the cross section for laser induced collision, as a function of the wavelength of the transfer laser is shown in Fig. 6. We note that the peak of the laser induced collision cross section occurs at about the $R = \infty$ wavelength of 4976.8 \AA (wavelengths are given in air). The half-power linewidth for the process is 14 cm^{-1} and the line has a slight asymmetry to the red. The linewidth of the transfer laser used in these experiments was 2 cm^{-1} .

The slight asymmetry to the red indicates that the van der Waals constant C_6 for the $\text{Ca}(6s^1S)$ target state is comparable in magnitude to that of the $\text{Sr}(5p^1P^0)$ storage state. This is consistent with a rough calculation. The linewidth of the process associated with the $\text{Ca}(5d^1D)$ target state is about 30% narrower than that for the $\text{Ca}(6s)$ state, and is also slightly asymmetrical to the red.

We have not yet properly calibrated the magnitude of these effects. The amplitude of the fluorescent signals obtained by the laser induced collisional process is about $1/500^{\text{th}}$ of that obtained by tuning the transfer laser to the two-photon absorption frequency of the $\text{Ca}(6s)$ level. The signal to background ratio is about five. If we assume theory to be correct, then at the power density of the transfer laser, the observed signal corresponds to a storage density in the $\text{Sr}(5p)$ level of about $10^{13} \text{ atoms/cm}^3$. This is roughly consistent with our estimates of population obtained by absorption probing. Over a total scan range of about 400 cm^{-1} , the peak

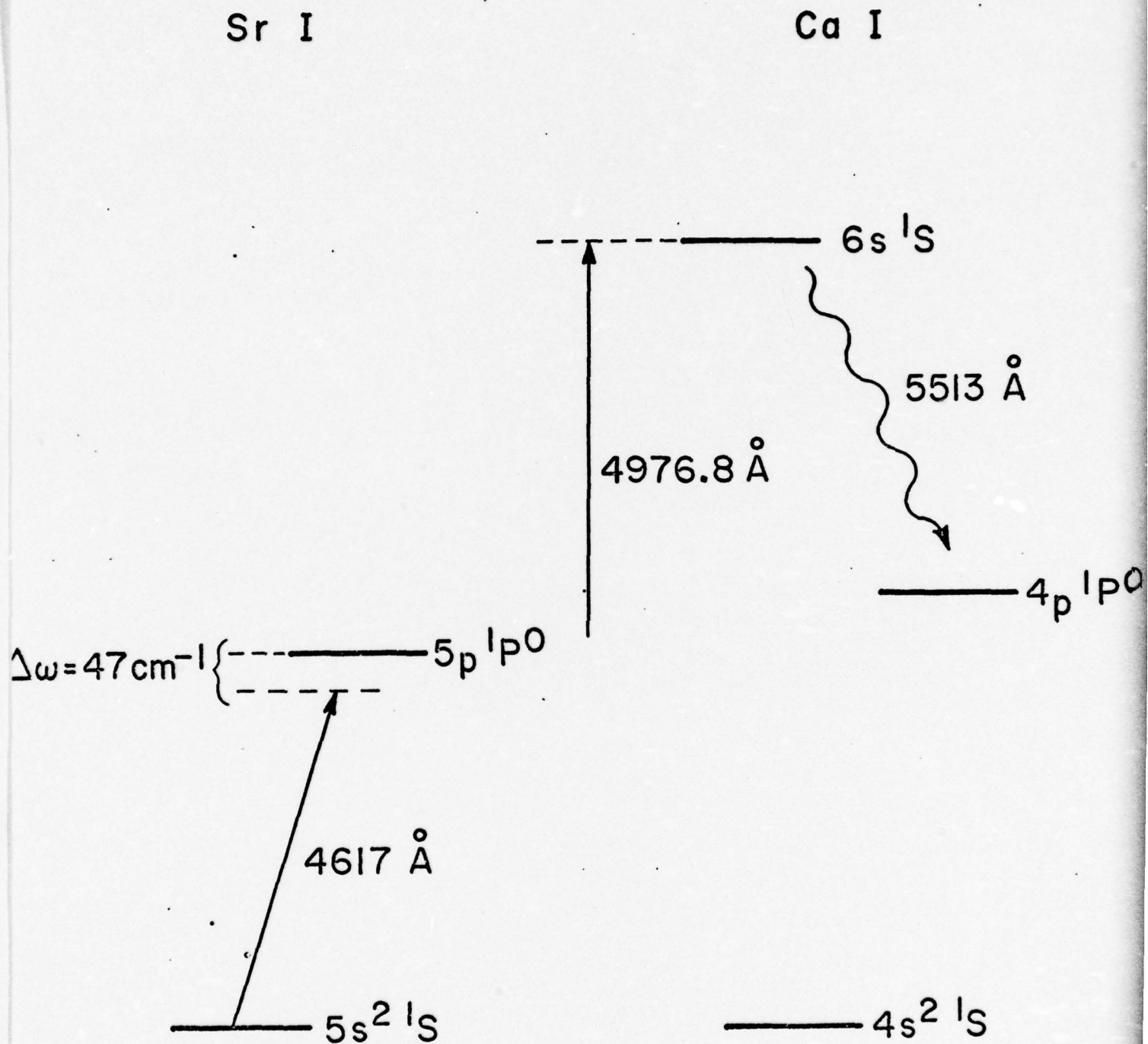


Fig. 5--Energy level diagram for the recent Sr-Ca induced collision experiment.

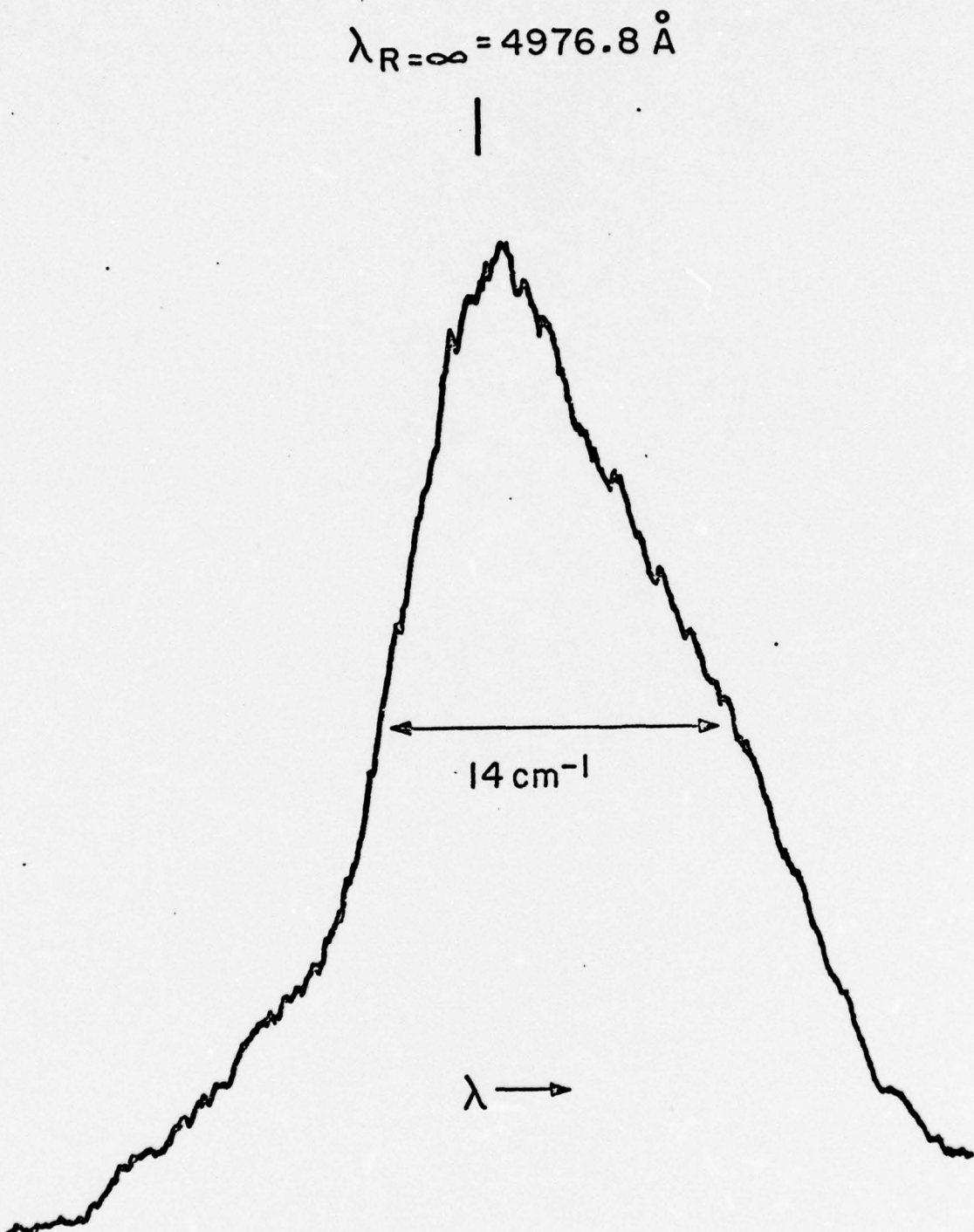


Fig. 6--Experimental results showing collision cross section as a function of transfer laser wavelength. The position of the $R = \infty$ wavelength is uncertain to 0.2 \AA .

shown in Fig. 6 is the only one which is not explained as either a two-photon summing process or as a direct atomic line excitation, followed by collision.

A possible alternate mechanism for the observed signal is two-photon absorption to the Ca(6s) state, where one of the photons result from spontaneous emission from the Sr(5p) level, and the second is furnished by the transfer laser. To eliminate this possibility we varied the density of an argon buffer gas from about 10^{17} to 10^{18} atoms/cm³. Over this range, no observable change was noted in the cross section vs. transfer laser linewidth (Fig. 6). Over this same range of argon pressure, the 50% transmission width of the resonance line varied by $\sqrt{10}$. Also, calculations indicate that such a two-photon absorption should be about 10^4 smaller than the observed signal.

Applications

I will now briefly describe a number of potential applications and devices which may result from collisional processes of this type. We first consider a radiative collision laser [1]. A schematic of a radiative collision laser is shown in Fig. 7. In a laser of this type energy would be stored in the radiatively trapped resonance line of Sr. During collision with a Tl atom, a Sr atom would be de-excited while a Tl would be excited from ground to the Tl 6p $^2P^0$ [1½] level. A photon at 7190 Å would experience gain rather than loss. The gain coefficient g is related to the collision cross section σ_c according to

$$g = \frac{N_A N_B \bar{V} \omega \sigma_c}{P/A} \quad (9)$$

where N_A and N_B are the number density of the two species. If we take $\sigma_c = 10^{-22} P/A$, $N_A = 10^{16}$ atoms/cm³, $N_B = 10^{19}$ atoms/cm³, $\omega = 10^{15}$ radians/sec, and $\bar{V} = 10^5$ cm/sec, we find a gain cross section of $g = 0.1 \text{ cm}^{-1}$. This number is somewhat optimistic for a typical system. A laser of this type may be of practical interest for two reasons: First, is the attractive possibility of radiatively trapped resonance line storage. Second, is the variable gain cross section provided by varying the number density of the second (ground state) species.

Though most of the discussion of this paper has been concerned with a single-photon transfer process, all ideas continue to hold for a multi-photon process. By storing energy in high lying states of atoms or ions,

RADIATIVE COLLISION LASER

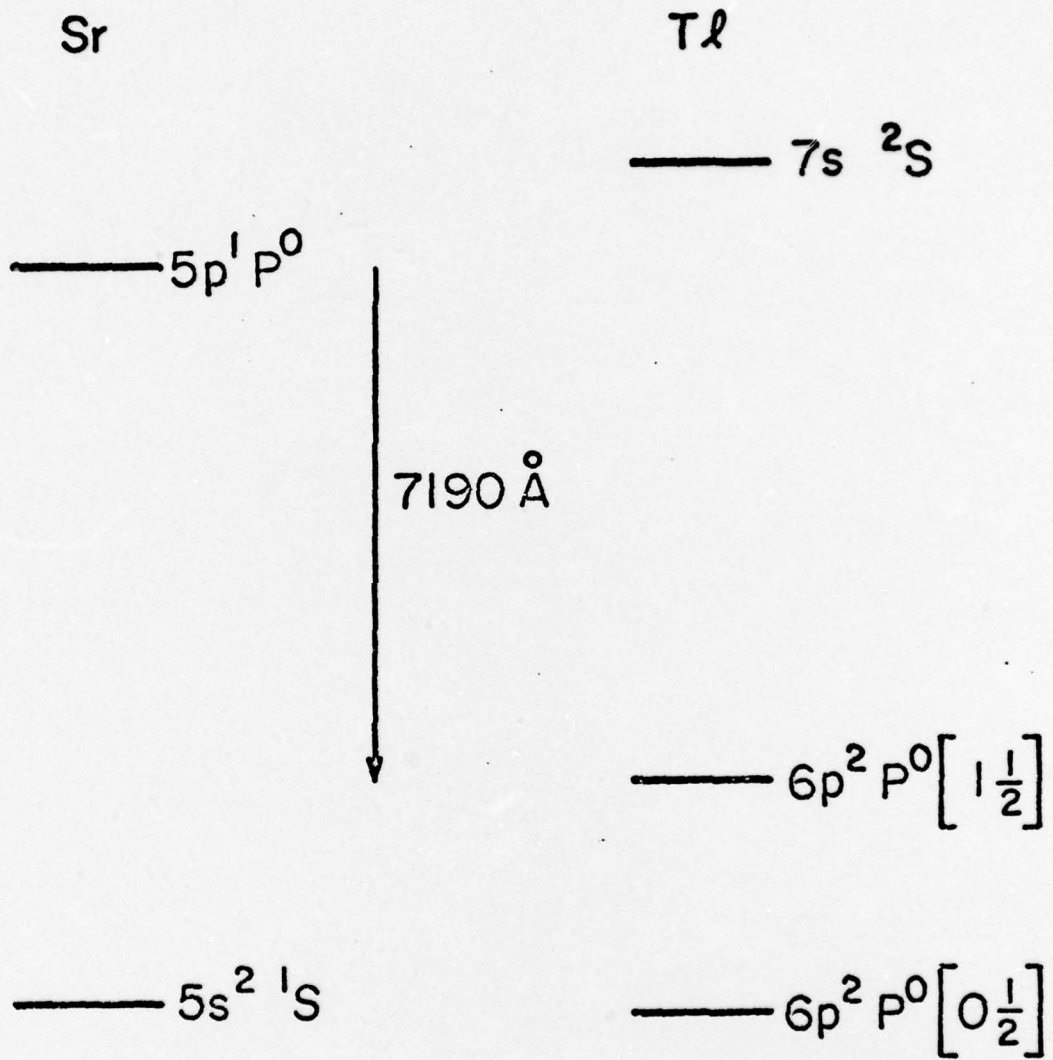


Fig. 7--Energy level diagram of a possible radiative collision laser.

and then using multi-photon processes with the intense VUV light sources now available, it should be possible to reach states to at least the 100 Å spectral region.

Coherent collisionally induced Raman processes such as that shown in Fig. 8 may be of interest for up-conversion of long wavelength radiation. This process is alternately described as a collisionally aided Stokes process which allows an output frequency higher than the input frequency, or alternately as an anti-Stokes process in a quasi-molecular system. The ability to demonstrate processes of this type will be dependent on achieving high number densities of the ground state species.

Other areas of application of these processes include the selective ionization of innershell electrons, laser induced charge transfer collisions, and perhaps radiative charge transfer lasers.

Laser induced collisions may someday allow one to direct the flow of energy and thus to influence reaction rates of general gas phase kinetic processes.

The authors acknowledge helpful discussions with David Bloom and Alan Gallagher. We wish to thank Mr. Ben Yoshizumi for help with the experiments reported here.

COHERENT RAMAN PROCESSES

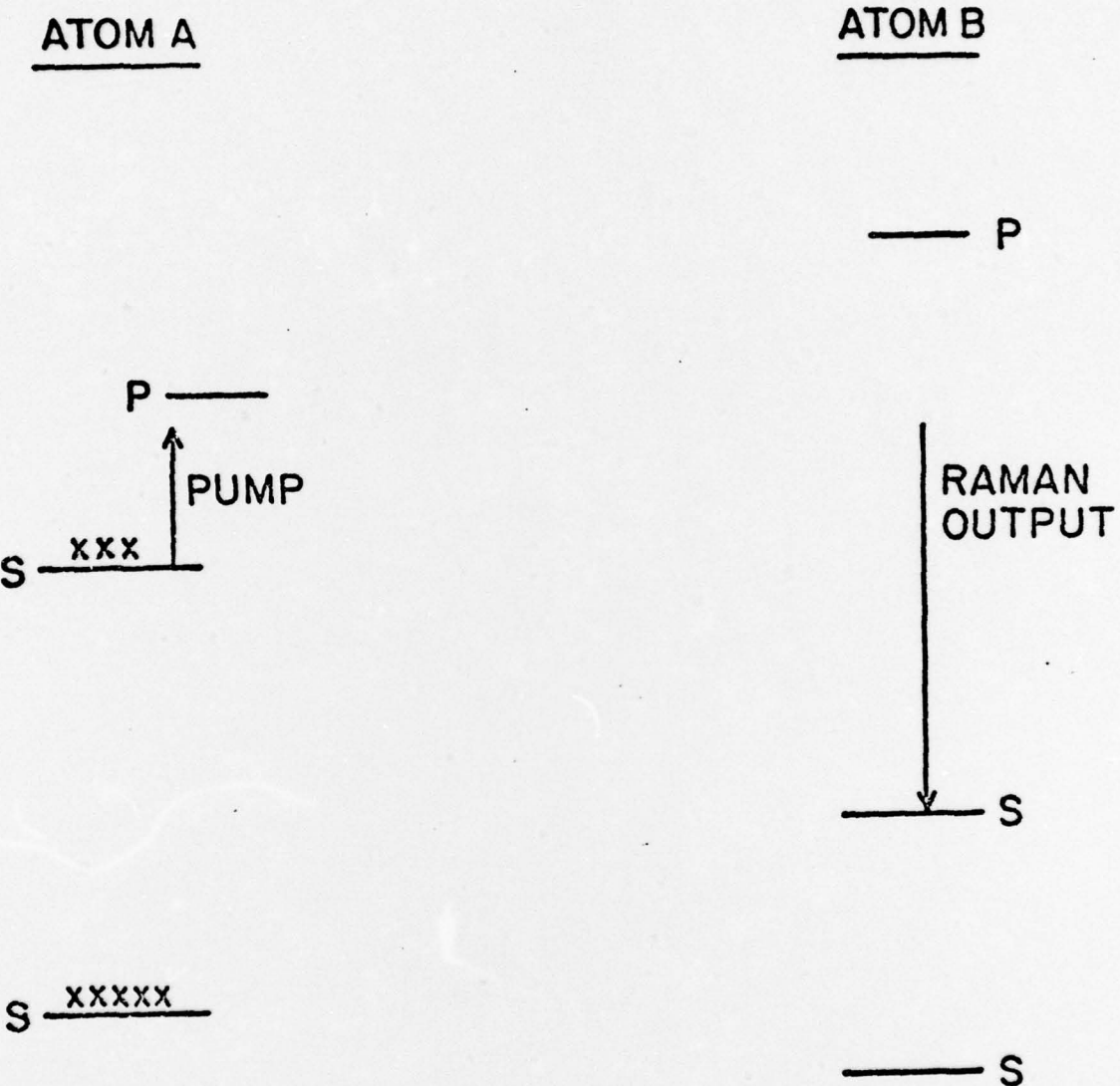


Fig. 8--In a coherent collisional Raman process gain is obtained at the Raman output frequency. Note that atom A need not be inverted, and that the frequency of the Raman output may be higher than that of the pumping frequency.

List of References

- * This work was jointly supported by the U.S. Office of Naval Research, the Advanced Research Projects Agency, and the Energy Research and Development Administration.
1. L. I. Gudzenko and S. I. Yakovlenko, *Zh. Eksp. Teor. Fiz.* 62, 1686 (1972) [*Sov. Phys. JETP* 35, 877 (1972)].
 2. S. E. Harris and D. B. Lidow, *Phys. Rev. Lett.* 33, 674 (1974), and 34, 172(E) (1975).
 3. M. G. Payne and M. H. Nayfeh, "Laser Enhanced Collisional Energy Transfer" (to be published).
 4. Sydney Geltman, "Theory of Laser-Stimulated Collisional Excitation Transfer" (to be published).
 5. Thomas F. George, Jian-Min Yuan, I. Harold Zimmerman, and John R. Laing, "Radiative Transitions for Molecular Collisions in an Intense Laser Field," *Disc. Faraday Soc.* No. 62.
 6. D. B. Lidow, R. W. Falcone, J. F. Young, and S. E. Harris, *Phys. Rev. Lett.* 36, 462 (March 1976).

List of Figures

1. Schematic of laser induced collision process. Energy is stored in the s state of atom A and may be rapidly transferred to the upper p state of atom B.
2. Virtual transition viewpoint of laser induced collisions. For flow of energy from the left- to the right-hand atom, the process is best considered as a virtual electromagnetic transition followed by a real collision. For the reverse process, we view the process as a virtual collision followed by a real transition.
3. Quasi-molecular viewpoint of laser induced collisions. A photon of frequency $\hbar\omega$ causes an electromagnetic transition between the initial and final state of the quasi-molecule.
4. Energy level diagram for Sr-Ca induced-collision experiment.
5. Energy level diagram for the recent Sr-Ca induced collision experiment.
6. Experimental results showing collision cross section as a function of transfer laser wavelength. The position of the $R = \infty$ wavelength is uncertain to 0.2 Å.
7. Energy level diagram of a possible radiative collision laser.
8. In a coherent collisional Raman process gain is obtained at the Raman output frequency. Note that atom A need not be inverted, and that the frequency of the Raman output may be higher than that of the pumping frequency.

Inelastic Collision Induced by Intense Optical Radiation*

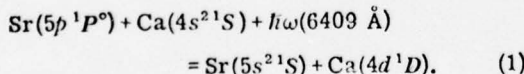
D. B. Lidow,[†] R. W. Falcone, J. F. Young, and S. E. Harris
Microwave Laboratory, Stanford University, Stanford, California 94305

(Received 30 December 1975)

A large cross section for inelastic collision is induced by an incident laser tuned to the frequency of the interatomic energy defect. We study energy transfer from the Sr $5p\ ^1P^o$ level to the Ca $4d\ ^1D$ level and measure a cross section for inelastic collision of $3 \times 10^{-16} \text{ cm}^2$ at a laser power density of $8.6 \times 10^6 \text{ W/cm}^2$ and a wavelength of 6409.0 \AA .

The cross section for inelastic collision between atoms is infinitesimally small if the energy defect ΔE is large with respect to kT . In this Letter we report the first observation of a process where a large cross section for inelastic collision is created by applying optical radiation at a frequency $\hbar\omega = \Delta E$. Energy transfer is initiated or "switched" by the presence of the optical radiation. Inelastic collision processes of this type have recently been predicted by Gudzenko and Yakovlenko¹ and by Harris and Lidow.²

We have observed this process in the system (Fig. 1)



Energy was first stored in the radiatively trapped $5p\ ^1P^o$ level of Sr I. This level was populated by two-photon pumping of the $5d\ ^1D$ Sr level, followed by radiative decay. Inelastic collision to the $4d\ ^1D$ level of Ca I was effected by a second laser beam at 6409 \AA .

During collision of an excited Sr $5p\ ^1P^o$ atom and a ground-state Ca $4s\ ^2S$ atom the strong dipole-dipole coupling of the $5p$ - $5s$ Sr transition

and the $4p$ - $4s$ Ca transition causes a virtual transition of the Ca atom. Absorption of a 6409 \AA

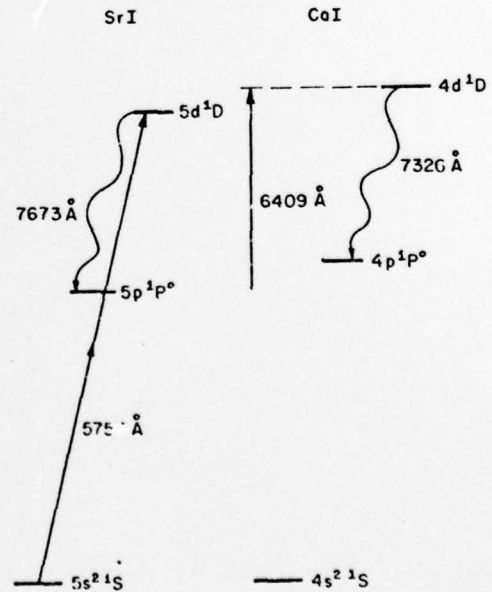


FIG. 1. Energy level diagram for Sr-Ca induced-collision experiment.

photon completes the Ca excitation. The process may thus be viewed as a virtual collisional excitation, followed by a real absorption.² Alternatively, and for the case described here equivalently, the process can be viewed as a free-free photon absorption of the Sr-Ca quasimolecule.¹ From either viewpoint, for dipole-dipole coupling, a maximum collision cross section is predicted when $\hbar\omega$ is equal to the interatomic transition frequency of the *infinitely separated* atoms ($R = \infty$). For incident radiation at the $R = \infty$ frequency, the predicted cross section for collision σ_c is given by²

$$\sigma_c = 2(\pi/\hbar^4)(\mu_{Sr}\mu_{Ca}\mu_{Ca^*}E/\bar{V}\rho_0\Delta\omega)^2, \quad (2)$$

where μ_{Sr} , μ_{Ca} , and μ_{Ca^*} are the magnitudes of the dipole matrix elements of the Sr 5s-5p, Ca 4s-4p, and Ca 4p-4d transitions, respectively; E is the strength of the applied optical field at 6409 Å; $\hbar\Delta\omega$ is the energy difference between the Sr 5p $^1P^o$ and Ca 4p $^1P^o$ levels; and \bar{V} is the average velocity. The quantity ρ_0 is the minimum impact parameter such that the integrated relative phase shift during transit is 1 rad, i.e.,

$$\frac{1}{\hbar} \int_{-\infty}^{+\infty} \frac{C_6}{R^6(t)} dt = \frac{3\pi\mu_{Sr}^2\mu_{Ca}^2}{8\hbar^2\bar{V}\Delta\omega\rho_0^5} = 1,$$

where C_6 is the energy-shift constant of the Sr 5p $^1P^o$ level. We neglect the comparatively small shift of the Ca 4d 1D level. Equation (2) includes only the dominant path of the perturbation calculation. For our experiments, $\mu_{Sr} = 3.0$ a.u., $\mu_{Ca} = 2.8$ a.u., $\mu_{Ca^*} = 0.95$ a.u., $\hbar\Delta\omega = 1954$ cm $^{-1}$, $\bar{V} = 6.6 \times 10^4$ cm/sec, $\rho_0 = 16.7$ Å, and $\sigma_c = (4.3 \times 10^{-23}$ cm $^4/W)P/A.$

A schematic of the experimental apparatus is shown in Fig. 2. The Sr-Ca heat-pipe-type cell was operated at a temperature of approximately 875°C and a zone length of 2 cm. The number densities of the Sr and Ca ground-state atoms

were determined by measuring the linewidths of their resonance absorption lines at 4608 and 4228 Å. These were $N_{Sr} = 8.0 \times 10^{16}$ atoms/cm 3 and $N_{Ca} = 3.8 \times 10^{16}$ atoms/cm 3 .

A Chromatix CMX-4 flashlamp-pumped dye laser produced the 5757-Å radiation for two-photon pumping of the Sr 5d 1D level. An incident power of about 1 kW was focused to a power density of 1.4×10^7 W/cm 2 . Emitted radiation at the 5d-5p Sr transition frequency was measured and used to estimate the population of the radiatively trapped Sr 5p $^1P^o$ level. Typically this density was about $N_{Sr}(5p\ ^1P^o) \approx 6 \times 10^{15}$ atoms/cm 3 . Two-photon pumping and radiative decay was used as the population mechanism of the Sr 5p $^1P^o$ storage level in order to avoid the necessity of directly applying radiation at the 5s-5p Sr frequency and thus possibly masking the desired collision process by a two-photon sum process to the Ca 4d 1D level.

Tunable radiation for inducing the collision process was provided by a Chromatix Model No. 1050 dye laser (Kiton Red) pumped with the second harmonic of the 1.12-μm line of a Q-switched neodymium-doped yttrium-aluminum-garnet laser. A peak power of 175 W in a 150-nsec pulse was focused to a power density of about 8.6×10^6 W/cm 2 and spatially overlapped with the 5757-Å pump beam. The relative timing of the two lasers could be adjusted over a range of several microseconds using a variable delay. Fluorescence of the Ca 4d-4p transition was measured and used to monitor the population of the Ca 4d 1D level.

The 5757-Å laser was first tuned to maximize the Sr 7673-Å radiation and thus the population of the Sr 5p $^1P^o$ level. With both lasers on, a maximum signal was measured with the transfer laser tuned to 6409.0 Å, as compared to the predicted ($R = \infty$) value of 6408.6 Å. (All wavelengths are given in air.) This is within the ±0.7-Å uncertainty of our wavelength calibration. The half-

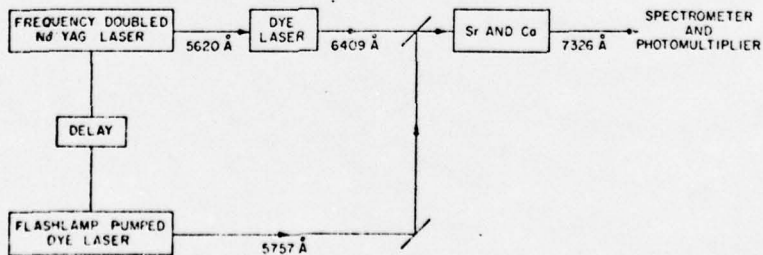


FIG. 2. Schematic of experimental apparatus.

power linewidth for transfer was $1.0 \pm 0.2 \text{ \AA}$. The linewidth of the Ca 7326- \AA fluorescence signal was limited by resolution. The 5757- \AA laser, by itself, produced some 7326- \AA fluorescence. A signal-to-noise ratio of about 50 was obtained by integrating over five pulses.

The ratio of the fluorescence output at the 7326- \AA Ca line to that at the 7673- \AA Sr line was 1:36. Allowing for the somewhat tighter focusing ($\sim \times 4$) of the 6409- \AA laser, as compared to the 5757- \AA laser, this fluorescence ratio indicates a collisional energy transfer of 11% for the excited Sr $5p^1P^o$ atoms to the Ca $4d^1D$ level. This transfer takes place during the 150-nsec pulse width of the 6409- \AA laser, indicating an induced cross section of $3 \times 10^{-16} \text{ cm}^2$. This cross section was linear in the incident power density. We estimate an experimental uncertainty of a factor of 3. For our power density of $8.6 \times 10^6 \text{ W/cm}^2$, Eq. (2) predicts a cross section of $3.7 \times 10^{-16} \text{ cm}^2$. The 6409- \AA transfer pulse could be delayed by about 0.5 μsec after the end of the 5757- \AA pulse before the 7326- \AA signal was significantly reduced. This is consistent with the estimated 0.5- μsec radiative trapping time of the Sr $5p^1P^o$ level.

We note that there are several Sr $6p^3P$ levels a few angstroms from coincidence with the Ca $4d^1D$ level. By tuning the transfer laser exactly to these levels, we ascertained that no direct collisional transfer was taking place.

Theory predicts that the optically induced collision cross section should continue to increase linearly with power density until $\sigma_c \approx \pi p_0^2$ and as the square root of power density thereafter. For the Sr-Ca system studied here $\pi p_0^2 = 8.8 \times 10^{-14} \text{ cm}^2$. Large energy transfer rates should thus be possible using this process.

The collisional process demonstrated here should be applicable to the direct measurement of interatomic potentials. Additional transfer peaks are expected at frequencies where the difference of the atomic potentials has zero slope, and at frequencies corresponding to turning points of the classical motion. Application to the construction of short-wavelength lasers is likely. Energy could be stored in a metastable atomic level, and by use of a short tunable optical pulse, collisionally switched to a radiative state of a second species. The inverse radiative process where lasing takes place between an excited state of one species and a lower state of a second species may be applicable to the construction of low-gain, high-energy lasers.

The authors very much appreciate the loan of the Chromatix Model No. 1050 dye laser. We thank Jonathan White and Ben Yoshizumi for experimental assistance, and Jim Newton for his cooperation.

*This work was jointly supported by the U. S. Office of Naval Research and the Advanced Research Projects Agency.

†D. B. Lidow gratefully acknowledges support from the Fannie and John K. Hertz Foundation.

¹L. I. Gudzenko and S. I. Yakovlenko, *Zh. Eksp. Teor. Fiz.* 62, 1686 (1972) [Sov. Phys. JETP 35, 877 (1972)].

²S. E. Harris and D. B. Lidow, *Phys. Rev. Lett.* 33, 674 (1974), and 34, 172(E) (1975).

³A. Lurio, R. L. DeZafra, and R. J. Goshen, *Phys. Rev.* 134, A1198 (1964); W. L. Wiese, M. W. Smith, and B. M. Miles, *Atomic Transition Probabilities*, U. S. National Bureau of Standards, National Standards Reference Data Series—22 (U.S. GPO, Washington, D.C., 1969), Vol. II.

ERRATUM

INELASTIC COLLISION INDUCED BY INTENSE OPTICAL RADIATION. D. B. Lidow, R. W. Falcone, J. F. Young, and S. E. Harris [Phys. Rev. Lett. 36, 462 (1976)].

Further investigations have indicated that the results reported in this Letter do not demonstrate a laser induced inelastic collision. The experiment was not able to distinguish between a Sr $4d^3D - 5p^3F$ transition at 6408.5 \AA and the Sr-Ca transfer predicted at 6408.6 \AA .

We have subsequently performed two new experiments in Sr-Ca which do not have such a wavelength coincidence.^{1,2} In both cases a laser induced collision was observed, and the transfer cross sections maximized at the expected interatomic wavelength.

¹S. E. Harris, R. W. Falcone, W. R. Green, D. B. Lidow, J. C. White, and J. F. Young, "Laser Induced Collisions," Proceedings of the International Conference on Tunable Lasers and Applications, Loen, Nordfjord, Norway, June 1976.

²R. W. Falcone, W. R. Green, J. C. White, J. F. Young, and S. E. Harris, "Observation of Laser Induced Inelastic Collisions," Phys. Rev. A (simultaneous submission).

APPENDIX B

Reproduction in whole or in part is permitted by the publisher for any purpose of the United States Government.

PHYSICAL REVIEW LETTERS

VOLUME 31

6 AUGUST 1973

NUMBER 6

Generation of Vacuum-Ultraviolet and Soft-X-Ray Radiation Using High-Order Nonlinear Optical Polarizabilities*

S. E. Harris

Microwave Laboratory, Stanford University, Stanford, California 94305

(Received 30 May 1973)

The harmonic or sum-frequency power generated in the last coherence length of a low-density atomic species is calculated subject to the condition that the applied electric field be bounded by the multiphoton absorption or ionization limit. It is shown that higher-order polarizations may equal or exceed lower-order polarizations. Calculations are given for generation at 1773 and 1064 Å in Xe, and at 236, 169, and 177 Å in Li⁺.

In recent years, picosecond-time-scale laser systems have evolved to the point where it is readily possible to produce focused optical pulses with power densities which are greater than the multiphoton ionization threshold of single atoms, and which at the same time have energy densities low enough that inverse bremsstrahlung (avalanche) ionization of the species does not occur.¹ By using the third-order nonlinear polarizability of low-pressure xenon, and operating at peak power densities which approach the multiphoton ionization limit ($P/A \approx 5 \times 10^{12} \text{ W/cm}^2$), picosecond laser pulses at 3547 Å have recently been used to produce third-harmonic radiation at a conversion efficiency of 3%.²

In this Letter, I consider the relative magnitude of the higher-order nonlinear optical polarizabilities; i.e., $\mathcal{P}^{(3)} \sim E^3$, $\mathcal{P}^{(5)} \sim E^5$, $\mathcal{P}^{(7)} \sim E^7$, etc.; where the applied electric field strength, E , is bounded by the condition that it not exceed the multiphoton absorption or ionization limit of the atom. It is shown, for many practical systems where the electronic transition frequencies

to ground are greater than the frequency of the applied laser fields, that at incident power densities which approach the multiphoton ionization limit, the higher-order polarizations may equal or exceed lower-order polarizations. There is also often a basic invariance, where the harmonic or sum-frequency power generated in the last coherence length of an atomic species is independent of the position and oscillator strengths of the intermediate levels, and of the order of the nonlinear polarizability involved. As a first experimental test of these ideas, Kung *et al.* have recently demonstrated the fifth-harmonic process 5320 Å → 1064 Å in low-pressure xenon.³

We consider an atomic system with certain transition frequencies to ground denoted by ω_{01} , $\omega_{02}, \dots, \omega_{0n}$. We assume that optical radiation at frequencies $\omega_1, \omega_2, \dots, \omega_n$ is applied to the system (for n th-harmonic generation $\omega_1 = \omega_2 = \dots = \omega_n$). We assume that a single path through the atomic levels dominates the nonlinear optical susceptibility. For a gas with N atoms/cm³, the dipole moment at the sum frequency $\omega_s = \omega_1 + \omega_2 + \dots + \omega_n$ is approximately given by⁴

$$\mathcal{P}^n(\omega_s) = N \frac{\mu_{01}\mu_{12}\dots\mu_{(n-1)n}\mu_{nn}}{h^n(\omega_1 - \omega_{01})(\omega_1 + \omega_2 - \omega_{02})\dots(\omega_s - \omega_{0n})} E(\omega_1)E(\omega_2)\dots E(\omega_n), \quad (1)$$

where μ_{ij} are the dipole matrix elements connecting the various levels (0 denotes ground, and is the

only level which is populated). We calculate the power density $P/A(\omega_s)$ which is generated in one coherence length at the sum frequency. (The coherence length is $L_c = |\pi/\Delta k|$, where Δk is the difference in the propagation vectors of the driving polarization and the free electromagnetic wave at ω_s .) Experimentally, this is the power density which will be generated when a Gaussian laser beam is focused to the center of a negatively dispersive media with a confocal parameter equal to L_c .^{5,6} We assume that the sum frequency ω_s is sufficiently close to ω_{on} that this transition, by itself, approximately determines L_c ; then

$$L_c = 2\pi\hbar(\omega_s - \omega_{on})/N\eta\omega_s\mu_{on}^2, \quad (2)$$

where $\eta = (\mu/e_0)^{1/2}$. From Maxwell's equations, the power density generated in one coherence length of atoms is $P/A(\omega_s) = (1/2\pi^2)\eta\omega_s^2[\mathcal{E}(\omega_s)]^2L_c^2$. Define $\gamma_{ij} = (\mu_{ij}E_j/\hbar\Delta\omega_j)^2$, where $\Delta\omega_j = \omega_{nj} - \omega_1 - \omega_2 - \dots - \omega_j$. Using Eqs. (1) and (2), the conversion efficiency from the highest applied frequency ω_n to the sum frequency ω_s is given by

$$\mathcal{E} = \frac{P/A(\omega_s)}{P/A(\omega_n)} = 4\gamma_{01}\gamma_{12}\dots\gamma_{n-2,n-1}\frac{\mu_{n-1,n}^2}{\mu_{on}^2}. \quad (3)$$

The maximum conversion efficiency to ω_s is determined by the maximum allowed value of $E(\omega_1), E(\omega_2), \dots, E(\omega_n)$. These are assumed to be limited by the n th-order absorption probability $W^{(n)}$ which, again subject to the assumption of a single dominant path, is given by^{7,8}

$$W^{(n)} = \hbar^{-2}\gamma_{01}\gamma_{12}\dots\gamma_{n-2,n-1}\mu_{n-1,n}\rho_n E^2(\omega_n), \quad (4)$$

where ρ_n is the density of states of the upper transition. Note that the single-photon cross section for absorption of ω_s by the transition ω_{on} is given by $\sigma_{on}(\omega_s) = \eta\omega_s\mu_{on}^2\rho_n/2\pi$. Using Eq. (4), Eq. (3) may be written

$$\mathcal{E} = \frac{\hbar\omega_s}{\sigma_{on}(\omega_s)} \frac{W^{(n)}}{[P(\omega_n)/A]} = \frac{\hbar\omega_s}{2\sigma_{on}(\omega_s)} \frac{1}{J(\omega_n)/A}, \quad (5)$$

where $J(\omega_n)/A$ is the incident energy density at the highest applied frequency ω_n . The second equality in Eq. (5) follows by multiplying numerator and denominator by the length of the laser pulse, Δt_p , and allowing the applied fields to increase until $W^{(n)}\Delta t_p = \frac{1}{2}$, i.e., 50% of the atoms are excited to the upper level. (It is assumed that Δt_p is shorter than the decay time of the upper level.) The quantity $\hbar\omega_s/2\sigma_{on}(\omega_s)$ is often termed the saturation energy density, and is that density which if incident from the outside would approximately saturate the transition.

Note that this conversion efficiency is independent of the order of the nonlinear polarizability, and also of the oscillator strengths and positions of the intermediate levels. If intermediate levels have smaller oscillator strengths or resonant denominators, the incident applied fields are allowed to increase to yield the same conversion efficiency.

The foregoing has assumed that the generated frequency ω_s is sufficiently close to some upper level ω_{on} , and that this level both determines the coherence length and most severely limits the allowable incident power density. More generally, the maximum allowable power density will be determined by multiphoton absorption to some other discrete level, or, most often, by multiphoton ionization to the continuum. Equation (3) still applies, but the maximum allowable E fields are now shown to be determined by the condition that

$$\gamma_{01}\gamma_{12}\dots\gamma_{q-2,q-1} = \frac{1}{8} \frac{\hbar\omega_s}{\sigma_{q-1,q}} \frac{1}{J/A(\omega_q)}, \quad (6)$$

where q denotes that level or point in the continuum which most severely limits the allowable fields. The quantity $\gamma_{01}\gamma_{12}\dots\gamma_{q-2,q-1}$ is then substituted into Eq. (3) to determine the conversion efficiency. [If $q=n$, then Eqs. (6) and (3) combine to give Eq. (5).]

Before applying the foregoing, two qualifications are in order. First, at the level of applied electric field strengths, Stark shifts may be significant. In principle, these can be included in the frequency denominators.⁹ In practice, allowing that the electric field is a free variable, the predicted conversion efficiencies are not very sensitive to the exact position of the upper atomic levels. There are also certain questions with regard to the applicability of the perturbation theory at these high field strengths. These same questions apply to multiphoton ionization theories,¹⁻⁹ which experimentally have proven to be reasonably accurate.

As a first example, consider the third-harmonic process 3547 Å → 1182 Å in xenon. To evaluate Eq. (6), I choose the four-photon path $5p^6[1S]0-6s[1\frac{1}{2}]1-6p[0\frac{1}{2}]1-7s[1\frac{1}{2}]2$ -continuum^{6,10} as that which will most severely bound the allowable incident power density. I assume unity oscillator strength for all transitions and estimate $\sigma_{7s\text{-continuum}}$ at $3 \times 10^{-19} \text{ cm}^2$.⁸ Then assuming an incident 30-ps pulse at 3547 Å yields $(P/A)_{\max} = 1.32 \times 10^{12} \text{ W/cm}^2$. At this density, Eq. (3) predicts a conversion efficiency of 0.34%. Experimentally, us-

TABLE I. Conversion efficiency and limiting power density for some higher-order nonlinear processes.

Process	Species and path	Limiting P/A (W/cm ²)	Conversion efficiency (%)
$3 \times 5320 \text{ \AA} \rightarrow 1773 \text{ \AA}$	Xe ^a , 5p-6s-5p-6s-6p-8d-c	1.94×10^{12}	0.084
$5 \times 5320 \text{ \AA} \rightarrow 1064 \text{ \AA}$	As above	As above	0.051
$5 \times 1182 \text{ \AA} \rightarrow 236 \text{ \AA}$	Li ^b , 1s-2p-1s-2p-3s-2p- 3s-4p-c	1.68×10^{15}	0.002
$7 \times 1182 \text{ \AA} \rightarrow 169 \text{ \AA}$	As above	As above	0.004
$15 \times 2660 \text{ \AA} \rightarrow 177 \text{ \AA}$	Li ^c , (1s-2p) ⁷ -(2p-3s) ⁷ -3p- 4d-c	3.47×10^{15}	4×10^{-7}

^a5p = 5p[¹S]0; 6s = 6s[¹S]0; 6p = 6p[¹D]2; 8d = 8d[¹D]3; c = continuum.^b1s = 1s[¹S]0; 2p = 2p[¹P]1; 3s = 3s[¹S]0; 4p = 4p[¹P]1; c = continuum.^c3p = 3p[¹P]1, others as in b.

ing tight focusing to the center of a xenon cell at a pressure of 3 Torr, a conversion efficiency of 0.9% has been measured.²

A number of other examples of the theory are summarized in Table I. The first two are concerned with generation of vacuum ultraviolet radiation in Xe. Assuming an incident laser pulse with a peak power of 10^8 W, then to exceed the multiphoton ionization limit we must focus to an area less than about 5×10^{-5} cm², and thus (at 5320 Å) to a confocal parameter less than 3.7 cm. For focusing to the center of a negatively dispersive media we set the coherence length L_c equal to the confocal parameter of the focus.^{5,6} For Xe in this region of the spectrum this will require an atom density between 10^{15} and 10^{16} atoms/cm³, and thus Xe pressures in the range of 0.1 Torr. At this pressure, and for a pulse length of 30 psec, avalanche breakdown would require a power density of about 5×10^{15} W/cm²¹¹; the assumption of multiphoton breakdown is thus well satisfied.

In recent weeks the processes $3 \times 5320 \text{ \AA} \rightarrow 1773 \text{ \AA}$ and $5 \times 5320 \text{ \AA} \rightarrow 1064 \text{ \AA}$ have been demonstrated experimentally. Conversion efficiencies are comparable and measurements will be reported subsequently.³

The final three examples in Table I are 5th-, 7th-, and 15th-order processes in singly ionized Li to generate radiation at 236 Å, 169 Å, and 177 Å. Ionization will be accomplished by the incident laser pulse. At ion densities of $\sim 10^{18}$ ions/cm³, recombination times are several nanoseconds,¹² and each atom need be ionized only once during the incident laser pulse. Because of the tight focus, this will require only about 10^{-5} of the incident pulse energy.

Even at its lower efficiency, the process 15-

$\times 2660 \text{ \AA} \rightarrow 177.3 \text{ \AA}$ may be an attractive early source of coherent soft-x-ray radiation. It makes use of a fortuitous coincidence with the 1s²[¹S]0-3p[¹P]1 transition of Li⁺ at 178.015 Å¹⁰ (2160 cm⁻¹ below the generated frequency). As a result of longer coherence lengths in this region of the spectrum, it is almost essential that coincidences of this type be utilized. Assuming an incident peak power of 10^{10} W, to attain the limiting power density, the laser must be focused to a confocal parameter = 0.43 cm. For L_c = confocal parameter, at an oscillator strength of 0.07 (equal to that of the comparable 1s-3p transition in He), this requires an ion density of 1.5×10^{19} ions/cm³. At this high density the condition on inverse bremsstrahlung ionization¹¹ is close to being violated.

By using sum-frequency processes, one photon of a tunable dye laser might be utilized to allow close frequency coincidences and thus to reduce the required ion or atom density. Sum-frequency processes might also be used to inject high-power, lower-frequency radiation and thus to reduce the required power density at the highest applied frequency. Phase-matching techniques^{2,6} may also be used to increase the conversion efficiencies of Table I.

The author gratefully acknowledges helpful and interesting discussions with H. Bebb, D. M. Bloom, G. C. Bjorklund, A. Gold, A. H. Kung, A. E. Siegman, E. A. Stappaerts, and J. F. Young.

*Work supported by the U. S. Office of Naval Research, the U. S. Air Force Cambridge Research Laboratories, and the U. S. Army Research Office.

¹G. S. Voronov and N. B. DeLone, Zh. Eksp. Teor. Fiz. Pis'ma Red. 1, 42 (1965) [JETP Lett. 1, 66 (1965)].

²A. H. Kung, J. F. Young, and S. E. Harris, Appl.

Phys. Lett. **22**, 301 (1973).

³A. H. Kung, E. A. Stappaerts, J. F. Young, and S. E. Harris, to be published.

⁴J. A. Armstrong, N. Bloembergen, J. Ducuing, and P. S. Pershan, *Phys. Rev.* **127**, 1918 (1962).

⁵J. F. Ward and G. H. C. New, *Phys. Rev.* **185**, 57 (1969).

⁶R. B. Miles and S. E. Harris, *IEEE J. Quantum Electron.* **9**, 470 (1973).

⁷H. B. Bebb and A. Gold, *Phys. Rev.* **143**, 1 (1966).

⁸V. M. Morton, *Proc. Phys. Soc., London* **92**, 301 (1967).

⁹L. V. Keldysh, *Zh. Eksp. Teor. Fiz.* **47**, 1945 (1964) [*Sov. Phys. JETP* **20**, 1307 (1965)].

¹⁰C. E. Moore, *Atomic Energy Levels*, U. S. National Bureau of Standards, National Standard Reference Data Systems-35 (U. S. GPO, Washington, D. C., 1971), Vols. 1 and 3.

¹¹M. Young and M. Hercher, *J. Appl. Phys.* **38**, 4393 (1967); A. V. Phelps, in *Physics of Quantum Electronics*, edited by P. L. Kelley *et al.* (McGraw-Hill, New York, 1966).

¹²H. R. Griem, *Plasma Spectroscopy* (McGraw-Hill, New York, 1964).

~~MICROWAVE LABORATORY~~

2178

STANFORD UNIVERSITY

Copy available to DDC does not
permit fully legible reproduction

